ANALYSIS OF THE LOWER TROPHIC LEVEL OF THE BLACK SEA ECOSYSTEM AFTER *MNEMIOPSIS LEIDYI* OUTBURST

A THESIS SUBMITTED TO
GRADUATE SCHOOL OF MARINE SCIENCES
OF
MIDDLE EAST TECHNICAL UNIVERSITY

BY

NUSRET SEVİNÇ

IN PARTIAL FULFILMENT OF THE REQUIREMENTS
FOR
THE DEGREE OF MASTER OF SCIENCE
IN
THE DEPARTMENT OF PHYSICAL OCEANOGRAPHY

SEPTEMBER 2010

Approval of thesis:

ANALYSIS OF THE LOWER TROPHIC LEVEL OF THE BLACK SEA ECOSYSTEM AFTER *MNEMIOPSIS LEIDYI* OUTBURST

Submitted by **NUSRET SEVİNÇ** in partial fulfilment of the requirements for the degree of **Master of Sciences in the Department of Physical Oceanography, Middle East Technical University** by,

Prof. Dr. Ferit Bingel _____
Director, **Graduate School of Marine Sciences**

Prof. Dr. Emin Özsoy _____
Head of Department, **Physical Oceanography**

Asst. Prof. Dr. Barış Salihoğlu _____
Supervisor, **Physical Oceanography Dept., METU**

Prof. Dr. Temel Oğuz _____
Co-Supervisor, **Physical Oceanography Dept., METU**

Examining Committee Members:

Asst. Prof. Dr. Barış Salihoğlu _____
Graduate School of Marine Sciences, METU

Prof. Dr. Temel Oğuz _____
Graduate School of Marine Sciences, METU

Asst. Prof. Dr. Bettina Fach Salihoğlu _____
Graduate School of Marine Sciences, METU

Prof. Dr. Semal Yemenicioğlu _____
Graduate School of Marine Sciences, METU

Dr. Yeşim Ak Örek _____
Graduate School of Marine Sciences, METU

Date: _____

I hereby declare that all information in this document has been obtained and presented in accordance with academic rules and ethical conduct. I also declare that, as required by these rules and conduct, I have fully cited and referenced all material and results that are not original to this work.

Name, Last Name: Nusret SEVİNÇ
Signature :

ABSTRACT

ANALYSIS OF THE LOWER TROPHIC LEVEL OF THE BLACK SEA ECOSYSTEM AFTER *MNEMIOPSIS LEIDYI* OUTBURST

SEVİNÇ, Nusret

M.S., Graduate School of Marine Sciences

Supervisor: Asst. Prof. Dr. Barış Salihoğlu

Co-Supervisor: Prof. Dr. Temel Oğuz

September 2010, 72 pages

The interactions between the main ecosystem components in the Black Sea and quantification of the response of different trophic levels to environmental changes was studied with a one-dimensional, vertically resolved (multi-layer), coupled physical-biogeochemical model. The simulations were used to better understand and quantify the influence of eutrophication and cold and warm winters on the ecosystem. In addition the prey-predator interactions, food competition and top-down control mechanisms were analysed in detail. The results revealed increase in biomass of all trophic levels in response to increased nutrient concentration. However, the eutrophication did not change the temporal evolution of the model compartments. The effects of cold and warm winters were represented as increased and decreased entrainment rates, respectively. In warm winter simulations decreased entraintment rates resulted in mixed layer depths that shallowed earlier than normal winters, this decreased the nutrient supply to upper layers and production in the upper layers. Lower production in the upper layers resulted in a shift of dominancy in the gelatinous carnivores from *Mnemiopsis leidyi* to *Aurelia aurita*. On the other hand, in cold winters, the mixed layer shallowed later than the normal winters. This shift in the shallowing of the mixed layer increased the nutrient supply to upper layers and production in the upper layers. A shift of dominancy in the gelatinous carnivores was observed also in cold winters. However,

Noctiluca scintillans biomass considerably increased by this change. In both cases, the lower trophic levels slightly influenced. Another important result indicated the top-down control of gelatinous carnivores in the system. Removing both of the gelatinous carnivores resulted in a decreased phytoplankton biomass. Two important guild structures revealed the food competition and prey-predator interactions. Reduction of gelatinous carnivores grazing rate on mesozooplankton increased the biomass of mesozooplankton and gelatinous carnivores, whereas decreased the biomass of microzooplankton. Reduction of gelatinous carnivores grazing rate on microzooplankton resulted in an increase of gelatinous carnivores and mesozooplankton biomass, a decrease on microzooplankton biomass. However, this change shifted the dominancy in gelatinous carnivores towards *Aurelia aurita*. In the other guild, the grazing pressure on microzooplankton exerted by mesozooplankton was reduced. This reduction decreased the biomass of mesozooplankton and phytoplankton, increased the biomass of microzooplankton. The reduction of grazing pressure exerted by mesozooplankton on phytoplankton resulted in an increase of microzooplankton biomass and a decrease of mesozooplankton and phytoplankton biomass. The physiological flexibility of the model compartments to adapt to the changing ecosystem structure and the ability to represent the environmental changes, imply a predictive potential of the model to forecast the effect of environmental changes on the marine ecosystems.

Keywords: Black Sea, ecosystem modeling, lower trophic level, gelatinous carnivores, environmental changes

ÖZ

KARADENİZ EKOSİSTEMİNİN ALT ENERJİ SEVİYESİNİN *MNEMIOPSIS LEIDYI* PATLAMASI SONRASI ANALİZİ

SEVİNÇ, Nusret
Yüksek Lisans, Fiziksel Oşinografi Bölümü
Tez Yöneticisi: Yrd. Doç. Dr. Barış Salihoğlu
Ortak Tez Yöneticisi: Prof. Dr. Temel Oğuz
Eylül 2010, 72 sayfa

Karadeniz ekosisteminin bileşenleri arasındaki etkileşimler ve farklı enerji seviyelerinin çevresel değişikliklere tepkisinin anlaşılması tek boyutlu, düşey çözünürlüklü (çoklu tabaka), birleştirilmiş fiziksel-biyojeokimyasal bir modelle çalışılmıştır. Ötrofikasyonun ve soğuk ve ılıman kışların ekosistem üzerindeki etkilerinin daha iyi anlaşılabilmesi için simülasyonlar yapılmıştır. Buna ek olarak, av-avcı etkileşimleri, besin rekabeti ve yukarıdan aşağıya uygulanan kontrol mekanizması detaylı olarak analiz edilmiştir. Sonuçlar artan besin konsantrasyonu sonucu bütün enerji seviyelerinde biyokütle artışı olduğunu göstermiştir. Ancak, ötrofikasyon model birleşenlerinin zamana bağlı dağılımlarını etkilememiştir. Soğuk ve ılıman kış etkileri entrainment hızı artırılarak ve azaltılarak gösterilmiştir. Ilıman kış simülasyonlarında azaltılan entrainment hızı karışık tabakanın normal kışlara gore daha erken sığlaşmasına neden olmuş, bu da üst tabakalara besin sağlanmasını ve üst tabakalardaki üretimi düşürmüştür. Üst tabakalardaki düşük üretim jelatinli etçillerdeki dominantlığın *Mnemiopsis leidyi*'den *Aureli aurita*'ya geçmesine neden olmuştur. Öte yandan, soğuk kışlarda karışık tabaka normal kışlara gore daha geç sığlaşmıştır. Karışık tabakadaki sığlaşmanın gecikmesi üst tabakalara besin sağlanmasını ve üst tabakalardaki üretimi artırmıştır. Soğuk kış simülasyonunda da jelatinli etçillerdeki dominantlık değişmiştir. Ancak, bu değişim neticesinde *Noctiluca scintillans* biyokütlesi farkedilir biçimde artmıştır. Her iki

koşulda da alt enerji seviyesi az etkilenmiştir. Bir başka önemli sonuç ise jelatinli etçiller tarafından, yukarıdan aşağıya uygulanan kontrolü göstermiştir. İki jelatinli etçili de sistemden çıkardığımız zaman fitoplankton biyokütlesi azalmıştır. İki önemli guild oluşumu besin rekabeti ve av-avcı etkileşimlerini ortaya çıkarmıştır. Jelatinli etçillerin mesozooplankton üzerindeki avlanma hızı azaltıldığında mesozooplankton ve jelatinli etçil biyokütleleri artmıştır, ancak microzooplankton biyokütlesi azalmıştır. Jelatinli etçillerin microzooplankton üzerindeki avlanma hızı azaltıldığında mesozooplankton ve jelatinli etçil biyokütleleri artmıştır, microzooplankton biyokütlesi azalmıştır. Ancak, bu değişim jelatinli etçillerdeki dominantlığı *Aurelia aurita*'ya çevirmiştir. Diğer guildde, mesozooplanktonun microzooplankton üzerindeki avlanma hızı azaltılmıştır. Bu azalış mesozooplankton ve fitoplankton biyokütlelerini azalmış, microzooplankton biyokütlesini artırmıştır. Mesozooplanktonun fitoplankto üzerindeki avlanma hızı azaltıldığında mesozooplankton ve fitoplankton biyokütleleri azalmış, microzooplankton biyokütlesi artmıştır. Model bileşenlerinin değişen ekosistem yapısına uyum sağlamasına yol açan fizyolojik esneklikleri ve çevresel değişiklikleri yansıtma becerileri, denizel ekosistemlerde çevresel değişikliklerin etkisini tahmin etme yönünde modelin bir potansiyelinin olduğunu göstermektedir.

Anahtar Kelimeler: Karadeniz, ekosistem modellemesi, alt enerji seviyesi, jelatinli etçiller, çevresel değişiklikler

To my family

ACKNOWLEDGEMENTS

I would like to thank to my supervisor Asst. Prof. Dr. Barış Salihoğlu and my co-supervisor Prof. Dr. Temel Oğuz for their guidance throughout the research and during the preparation of this work.

I am also sending my sincere gratitude to Asst. Prof. Dr. Bettina A. Fach Salihoğlu and Dr. Sinan Hüsrevoğlu for their help on programming.

Thanks to the ecosystem modellers group for their ideas and contributions.

I would like to thank to Dr. Yeşim Ak Örek and my colleagues in SETÜSTÜ for their moral support.

Finally I would like to thank to the staff and members of METU IMS and R/V Bilim2 for providing such beautiful facilities to work with.

TABLE OF CONTENTS

LIST OF TABLES

TABLES

LIST OF FIGURES

FIGURES

1 INTRODUCTION

The Black Sea, one of the largest semi-enclosed basins, is connected with the Mediterranean Sea by the Turkish Straits System (the Bosphorus and Dardanelles Straits and the Sea of Marmara). It has experienced crucial environmental degradation within the last four decades. Anthropogenic nutrient loading, climatic oscillations, introduction of invasive gelatinous carnivores and overfishing are the main reasons for the environmental crisis. Such an environmental crisis is very important and needs to be studied, since, the Black Sea has economically important fish stocks for the 6 bordering countries.

1.1 Physical Properties of the Black Sea

The Black Sea has a surface area of 423000 km^2 and a total volume of 547000 km^3. It has a maximum depth of 2212 m. The topographic variations around its periphery are very strong. The only major shelf is the northwestern shelf, which occupies %20 of the total area. The major river discharges are from Europe's three largest rivers, the Danube, the Dnieper and the Dniester to the Northwestern shelf, and the Don and the Kuban rivers to the Eastern Black Sea.

Vertical mixing of the water column in the Black Sea is limited to the upper layer down to a permanent halocline. The permanent halocline separates the water in the upper 150 meters from the intermediate and deep water. This physical characteristic of the Black Sea makes it one of the biggest meromictic basins in the world (Sorokin, 1983).

The physical characteristics of the upper layer change seasonally. In winter, the upper layer water mass is well mixed and homogenized up to 50 m depth in response to intensified wind stress (Oguz et al., 2005). This mixed layer is identified by temperature around 5-6 ^oC, salinity around 18.5-18.8 and density around 14.5 kg m^{-3} (Krivosheya et al., 2002). In spring, warm and mild winds stratify the surface water and trap the cold water generated in winter below the seasonal thermocline. The upper water mass up to 20 m depth is well mixed in spring and summer. This mixed

layer is characterized by temperature around 25 ^{o}C, salinity around 18 and density around 10-11 kg m^{-3} (Oguz et al., 2005). The depth of the euphotic zone in the interior basin is around 50-60 m (Sorokin, 1983).

The intermediate and deep water masses below the halocline is almost vertically uniform throughout the year. The physical characteristics are defined by temperature around 9 ^{o}C, salinity around 22 and density around 17 kg m^{-3} (Murray et al., 1991).

The upper layer circulation in the Black Sea can be described by three important systems (Oguz et al. 1993). They are the Rim Current system around the periphery, an interior cell composed by two or more cyclonic gyres and a series of quasi-stable anticyclonic eddies on the coastal side of the Rim Current. These quasi-permanent features, however, show some seasonal and interannual changes. In winter months, an organized two-gyre system is observed in the interior cell. This organized system disintegrates into a series of interconnecting eddies in the summer and autumn months (Korotaev et al., 2003).

On the coastal side of the Rim Current, the Sevastopol, Batumi, Crimean, Sakarya, Sinop, Caucasian and Bosphorus are the well known quasi-permanent anticyclonic eddies (Oguz et al., 1998c).

1.2 Chemical Properties of the Black Sea

The meromictic characteristic of the Black Sea inhibits mixing between the oxygen containing upper layer waters and water below the halocline. This results in anoxic conditions below the halocline (Sorokin, 1983).

Almost all of the biological production takes place in the upper layer waters of the Black Sea (Oguz et al., 2005). This is due to the shallow euphotic zone with a thickness of around 50-60 m. This fact causes a high chemical activity in the upper layer.

The nutrient concentrations in the surface mixed layer waters are changing seasonally and are mainly at low levels in the interior basin. In winter, the nutrients stocks in the euphotic zone are renewed from the nutricline through upwelling, vertical diffusion and entrainment processes. Below the mixed layer, at the deeper parts of the euphotic zone, nitrate concentrations are high due to nitrate recycling and continuous supply from the nutricline (Oguz et al., 2005).

The maximum nitrate concentrations measured at the deeper parts of oxic layer ranges between 6 to 9 μM. The greatest values are observed in the cyclonic gyres. Vertical distribution of phosphate in the oxic layer is very similar to nitrate profiles, but the concentration is lower and between 0.8 to 1.2 μM (Bingel et al., 1993). Dissolved ammonia concentration is between 0.1 to 0.3 μM in the surface waters (Codispoti et al., 1991).

In the oxic layer, %90 of the sinking particles are remineralized and resupplied back to the productive euphotic zone (Oguz et al., 2005). The small fraction of sinking material lost to anoxic layer is compensated mainly by the anthropogenic nutrient flux from the River Danube, as well as nitrogen fixation from the atmosphere (Cociasu et al., 1996).

1.3 Biological Properties of the Black Sea

Primary production in the Black Sea has an annual cycle of three peaks. The first peak is the spring bloom, which occurs from February to March. The second peak is in the summer, from April to May. The third peak occurs in autumn from August to September. During the spring bloom, primary production in the interior part of the basin is higher than in coastal parts. This is due to the difference in the process of nutrient transport to the productive area (Stelmakh et al., 1998).

In the summer, since the vertical transport of nutrients to the photosynthetically active region decreases, phytoplankton utilize the available nutrients, and the solar radiation is high, the diurnal assimilation number of the phtoplankton increases, thus, the euphotic zone enlarges. Most of the primary production occurs in the deeper part

of the enlarged euphotic zone. In autumn, a small phytoplankton bloom occurs. November - December period is the poorest in production (Stelmakh et al., 1998).

Dinoflagellates, diatoms, phytoflagellates, coccolithophorids, Silicoflagellates and flagellates are the most dominant phytoplanton groups in the interior basin (Nesterova et al., 2008). In summer and autumn, diatoms are the main dominant group, whereas in spring, the dominancy shifts to dinoflagellates. Phytoflagellates costitute more than 30% of the phytoplankton group throughout the year (Nesterova et al., 2008).

The development of zooplankton biomass in the Black Sea follows the phytoplankton structure, since phytoplankton constitutes most of the zooplankton's diet. Microzooplankton (<0.2 mm) and mesozooplankton (0.2 – 3 mm) communities consist the second trophic level in the Black Sea ecosystem (Oguz et al., 2001a).

The microzooplankton community represents heterotrophic flagellates (e.g. *Noctiluca scintillans* and ciliates. The mesozooplankton community consists of omnivores and carnivores. Copepods, cladocerans and appendicularians are represented as the omnivorous group. The carnivorous group consist of *Aurelia aurita*, *Mnemiopsis leidyi* and *Beroe ovata* (Oguz et al., 2001a; Shiganova et al., 2008) In the interior basin, *Palacalanus parvus*, *Pseudocalanus elongatus*, *Calanus euxinus* and *Parasagitta setosa* are the most dominant omnivorous mesozooplankton species (Shiganova et al., 2008).

Noctiluca scintillans biomass in the Black Sea changes rapidly with food competition against gelatinous carnivores and climatic conditions. Currently, *Noctiluca scintillans* biomass is at low quantities (< 1 g m^{-2}). *Noctiluca scintillans* imply strong blooms in late-spring or autumn (Shiganova et al., 2008).

The biomass of medusae *Aurelia aurita* starts producing during spring months, when the food is abundant, and the maximum concentration (0.4 g m^{-2}) is maintained in summer (Araskevich et al., 2008b). However, the biomass decreases rapidly in fall, probably due to low food abundance and sensitivity to colder temperatures (Oguz et al., 2001a).

The biomass of ctenophore *Mnemiopsis leidyi* is at its minimum in winter. With the start of spring, *Mnemiopsis leidyi* biomass develops and reaches a maximum (0.4 g m^{-2}) in summer. However, in autumn, it's biomass decreases to the winter values (Araskevich et al., 2008b).

1.4 Environmental Changes in the Black Sea

In the past four decades, high anthropogenic and climatic stress was observed in the Black Sea. Eutrophication and strong decadal climatic perturbations are the main factors which result in this stress (Oguz et al., 2009b).

1.4.1 Eutrophication

Eutrophication is described by Oguz et al. (2009b), as the undesirable disturbances in ecosystem functioning due to anthropogenic enrichment by nutrients and subsequent accelerated growth of algae and higher life forms.

Excessive nutrient loading to the Black Sea was observed in the northwestern shelf in early 1970s. Danube river discharged %80 of the river-based nutrient supply (derived by agriculture, industry, urban settlements) in 1970s and 1980s (Oguz et al., 2009a).

In 1990s, with the closure of ecologically ineffective large agricultural facilities, reduced phosphate in detergents and nutrient removal by waste water treatment plants, total phosphate and dissolved inorganic nitrogen load into the Black Sea reduced (Oguz et al., 2009b).

In the present decade, western coastal waters of the northwestern shelf is still suffering from dissolved inorganic and organic nitrogen loading. However, the interior basin responded to the decline in dissolved inorganic nitrogen in the overall basin and reduced the peak nitrate concentration of 6 μM in 1990s to 4 μM (Oguz et al., 2009b).

1.4.2 Decadal Climatic Perturbations

Climatic perturbations effect the Black Sea ecosystem mainly via the oscillating sea surface temperature (Yunev et al., 2007). Other means of climatic perturbations effects are anomalies in precipitation, solar radiation, heat flux and wind stress. These anomalies lead to changes in nutrient cycling, primary production and prey-predator interactions via influencing the circulation, water column stratification, vertical mixing, downwelling and upwelling (Oguz T., 2005b).

Cumulative sum method performed by Shapiro et al. (2010) revealed regime shifts in years 1927, 1966, 1968, 1986 and 1997. 1920s were warm years with some positive and negative fluctuations of air temperature. The period from 1940 to 1960 showed a cooling trend, again with some fluctuations. However, from 1960 to 1968, a drastic warming was observed, followed by a slow cooling until 1986 (Shapiro et al., 2010)

The periods from 1985 to 1987 and 1991 to 1993, are the coldest periods of the last century with winter-mean mixed layer temperatures as low as 7.2 ºC. The warm period from 1987 to 1991 is even cooler by 0.5 ºC than the coldest temperature of the previous warm cycle in 1970s. After 1995, the Black Sea temperature entered a warming cycle at a rate of 0.2 ºC per year until 2002 (Oguz T., 2005b).

1.5 Long-Term Ecosystem Changes in the Black Sea

The Black Sea has suffered from severe ecological changes during the last four decades. The factors that play a role in these changes are: excessive nutrient input, outburst of alien ctenophore species *Mnemiopsis leidyi*, overfishing and climate impact (Oguz et al., 2007).

Excessive nutrient loading increased the percentage of dinoflagellates in the harmful algal blooms during 1980s and 1990s, whereas the percentage of diatoms decreased (Bodeanu, 1993; Moncheva and Krastev, 1997). The summer blooms of phytoplankton occured regularly in addition to the regular spring blooms (Oguz et al., 2007). Summer – Autumn mean phytoplankton biomass in the interior basin

increased from 1 g m^{-2} to 2 g m^{-2} in 1960s, to 10 g m^{-2} in 1970s and to 20 g m^{-2} in 1980s (Mikaelyan, 1997).

In early 1980s, the system was dominated by opportunistic species *Noctiluca scintillans* and gelatinous carnivore *Aurelia aurita* (Shiganova et al., 2008). In late 1980s, the outburst of gelatinous carnivore *Mnemiopsis leidyi* reduced the mesozooplankton community as well as the fish egg and larvae (Shuskina et al., 1998). The outburst of *Mnemiopsis leidyi*, also decreased the *Noctiluca scintillans* and *Aurelia aurita* biomass abruptly (Shiganova et al., 2008).

In 1998, a new invasive gelatinous carnivore *Beroe ovata* introduced into the system (Konsulov and Kamburska, 1998). Biomass development of *Beroe ovata* helped recovery of the system, decreased *Mnemiopsis leidyi* biomass, and increased *Aurelia aurita* and *Noctiluca scintillans* (Shiganova, 2000).

Oguz (2005a) concludes that the anthropogenic forcings of the excessive nutrient loading from the rivers during 1970s resulted in a bottom-up control of the ecosystem and led to deposition of excess nutrients within the subsurface water layers. Top-down control of the ecosystem was imposed by overfishing and population outbursts of the gelatinous carnivores in 1980s. It exerted decadal scale variations and resulted in order-of-magnitude changes in the species biomass.

1.6 Previous Modeling Studies

Modeling studies on the ecosystem of the Black Sea are very limited and are being done only for two decades.

Lebedeva and Shuskina (1994) studied the structure and functioning of the plankton community of the interior part of the Black Sea before and after the outburst of *Mnemiopsis leidyi*. They developed a one-dimensional mixed layer model representing the pelagic lower trophic level of the food web. Phosphate was used as the limiting nutrient.

Eeckhout and Lancelot (1997) developed a one-dimensional model with the purpose of studying the role of nutrient enrichment on destabilization of the Northwestern shelf ecosystem within the last three decades. Carbon, nitrogen, phosphorus and silicate cycles, diatoms, nanophytoplagellates, bacteria, microzooplankton, copepods, dissolved and particulate organic matter were the compartments of the model. The model was extended to study the response of increased antropogenic nutrient load by including gelatinous organisms.

Cokacar (1996) used different variations of Fasham's (1990) model to simulate the regional ecosystems of the Black Sea. A series of simulations were made using model ranging from four compartment PZND model to a 9 compartment size-fractioned model for ten different regions in the Black Sea.

Salihoglu (1998) applied a three dimensional, coupled physical-biological model to simulate the plankton productivity and nitrogen cycling in the upper layer water column of the Black Sea. The model's vertical structure was three layered and the limiting nutrient was nitrogen. Diatom and flagellate phytoplankton groups, microzooplankton, mesozooplankton, labile pelagic detritus, nitrate and ammonium were the compartments of the model. A major finding of the model results is quantitative demonstration for the necessity of the second and third layers for successful simulations of the summertime subsurface chlorophyll layer.

Oguz et al., (1996) developed a biologically simple model which couples the upper-layer dynamics with the ecosystem dynamics. Phytoplankton, zooplankton, detritus, nitrate and ammonium were the components of the model. 150 m of the upper layer water column of the central Black Sea was modeled with a 3 m grid spacing. Oguz et al., (1998a) extended the previous model by defining two seperate phytoplankton (diatoms and flagellates) and two seperate zooplankton groups (microzooplankton, mesozooplankton), in order to obtain more realistic biological production. With the addition of macrozooplakton compartment, Oguz et al., (1998b) represented the gelatinous carnivores in the models. Bacterioplankton and dissolved organic nitrogen compartments also added to the model.

Oguz et al., (2001b), compared the results of a multi-level model with multi-layer alternatives in order to investigate the feasibility of using a relatively simpler model and look to its optimum vertical configuration. The phytoplankton seasonal cycle of the Black Sea was simulated using the model. Same biological settings were used in the simulations. The key conclusion of this study is that, despite the simple vertical configuration, multi-layer models emerge as a practical alternative tool to more complex multi-level models.

More studies done with the similar model structure (Oguz et al., 1999, 2000, 2001a, 2002; Oguz and Salihoglu, 2000; Oguz, 2005a,b).

1.7 Purpose of This Study

In this study, a one-dimensional, coupled physical-biological model, developed by Oguz et al., (2001b), is used to investigate the top-down control exerted by the gelatinous carnivores, effect of the anthropogenic nutrient loading, and the effect of climatic variations on the Black Sea pelagic food web. The aim of the study is to better understand and quantify the influence of eutrophication, cold and warm winters on the ecosystem and the prey-predator interactions, food competition and top-down control mechanisms. The model has a simplified physical vertical structure, in which the upper 100 m of the Black Sea is represented by three interactive layers.

2 MATERIAL AND METHOD

The structure of one-dimensional, vertically resolved, coupled physical-biogeochemical model is described in this section. Following this, the biogeochemical and physical structures of the model is described in seperate subsections. The numerical procedure and initial conditions are described in subsection 4. This is followed by the descriptions of reference parameter setting and the parameter settings of the simulations.

2.1 Model Description

The model used in this study is developed by Oguz et al. (2001b). The model applies for the conditions outside the northwestern shelf and uses nitrogen as the main limiting nutrient for the interior Black Sea basin. The model approximates the vertical biogeochemical structure of the upper layer by three interactive layers (Fig. 1). The model solves a set of equations representing the ecosystem and layer Dynamics.

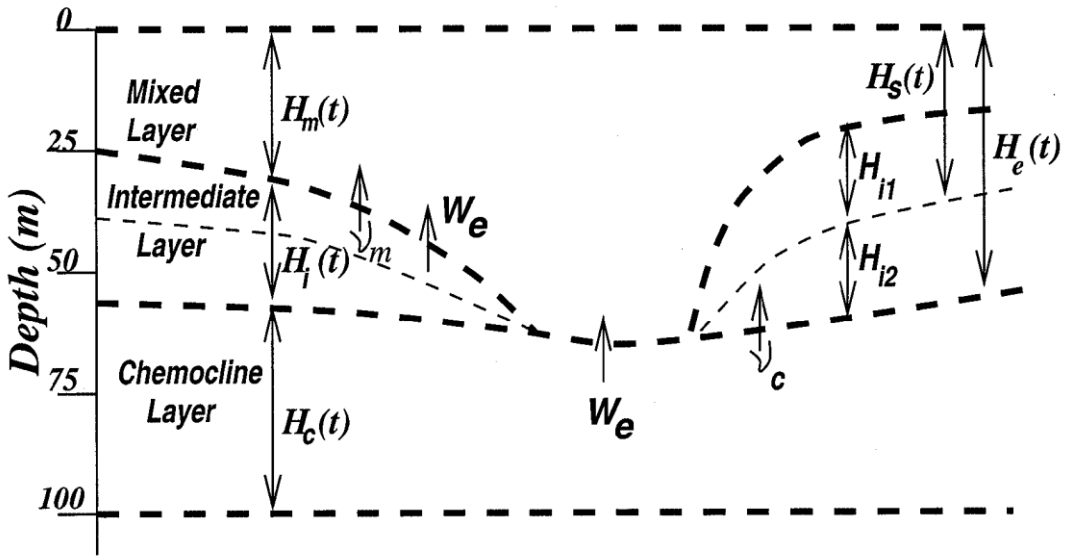

Figure 1. The schematic diagram of the vertical structure of the model (after Oguz et al. (2001b)).

2.2 Physical Structure of the Model

The first layer is the mixed layer, seasonally varying in depth. This layer is followed by the intermediate layer which has a seasonally varying thickness. These two layers represent the euphotic zone. Intermediate layer is the lower part of the euphotic zone, below the seasonal thermocline. The third layer is the chemocline zone, representing the aphotic zone of the upper layer water column up to the anoxic interface (Fig. 1).

The chemocline zone acts as a nitrogen pool where the sinking particulate materials are remineralized and converted to inorganic form. The nutrients in this layer is then made available to the euphotic zone by means of vertical diffusion and entrainment. Primary production occurs in the first two layers.

The dynamic mixed layer depth changes with the entrainment rate. The entrainment rate W_e is computed according to Kraus-Turner type bulk mixed layer dynamics as in Niiler and Kraus (1977) by:

$$\theta(W_e)W_e b_m H_m = 2mu_*^2 + H_m B_0[1 - \lambda\theta(\mathrm{W_e})] \quad (1)$$

where $u_*^2 = |\tau_0|/\rho_0$ denotes the friction velocity square with $|\rho_0|$ representing magnitude of the wind stres, $b_m = g(\frac{\Delta\rho}{\rho_0})$ is the bouyancy at the base of the mixed layer, and B_0 is the total bouyancy flux through the surface, varies temporally due to the total surface heat flux.

By assuming that deeper part of the mixed layer below euphotic zone is biologically inactive, the maximum thickness of the mixed layer is limited by the euphotic zone. The thickness of the euphotic zone is determined by the 1 % light level. This level is computed in the model for a given value of water extinction coefficient. The intermediate layer thickness is the difference between euphotic zone thickness and mixed layer thickness. In strong mixing periods, the intermediate layer vanishes and the model becomes two layered.

The thickness of the chemocline layer is the difference between total upper layer water column (taken as 100 m) and the euphotic zone.

2.3 Biological Structure of the Model

The lower trophic level of the pelagic food web is represented in 11 compartments. These compartments are; small phytoplankton (P_s), diatom (P_{da}), dinoflagellate (P_{di}), microzooplankton (Z_{mi}), mesozooplankton (Z_{me}), heterotrophic dinoflagellate *Noctiluca scintillans* (N_s), gelatinous carnivores *Aurelia aurita* (Z_a) and *Mnemiopsis leidyi* (Z_m), labile pelagic detritus (D), nitrate (N) and ammonium (A). The reason of having 3 different phytoplankton and 2 different zooplankton groups, is the difference in size and bloom timing between the groups. Interactions between the model compartments are shown in Figure 2.

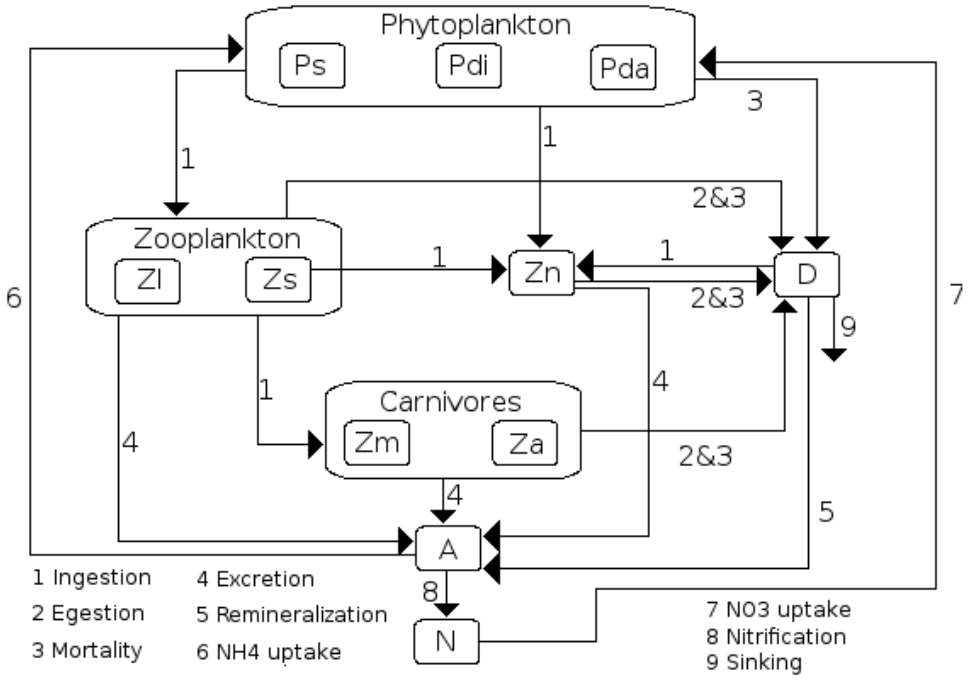

Figure 2. Interactions between the model compartments. Arrows indicate the direction of nitrogen transfer between model compartments. The ecosystem variables are annually averaged within the water column (0-100 m). Abbreviations on the flow chart are: A- Ammonium, N- Nitrate, D- Detritus, P_s- Small phytoplankton, P_{di}- Dinoflagellates, P_{da}- Diatoms, Z_s- Microzooplankton, Z_l- Mesozooplankton, Z_n- *Noctiluca scintillans*, Z_m- *Mnemiopsis leidyi* and Z_a- *Aurelia aurita*.

This food web structure of the model is similar to that given by Oguz et al., (2000, 2001a,b) except for the addition of another phytoplankton group and the absence of dissolved organic nitrogen and bacterioplankton compartments. The complex bacterial dynamics are ignored for simplicity.

The temporal variations of all biological variables change occur via two mechanisms; the biological sources and sinks, and the vertical transports (e.g. entrainment, diffusion and sinking), and expressed by:

$$\frac{\partial F_j}{\partial t} = X_j(F) + R_j(F) \tag{2}$$

where *t* is time, ∂ is the partial derivative, F_j represents the concentration or biomass of any variable in layer *j*. *R(F)* and *X(F)* denote, respectively, the biological source-sink terms and the vertical transports.

The three-layer model allows mixing and material exchanges across the layer interfaces through entrainment and diffusion. The particulate organic material sinking is also treated as in the form of interfacial transfers.

The net transport X_m across the base of the mixed layer is then expressed as:

$$X_m = [(\theta(W_e)W_e + v_m)(F_i - F_m) - w_s F_m/H_m] \tag{3}$$

where the Heaviside step function θ is defined by $\theta(W_e) = 1$ and $\theta(-W_e) = 0$ if $W_e > 0$. v_m denotes the diffusion rate across the base of the mixed layer.

The net transport for the intermediate layer, X_i, involves diffusion and sinking fluxes across its lower and upper boundaries:

$$X_i = [v_c(F_c - F_i) - v_m(F_i - F_m) - w_s(F_i - F_m)]/H_i \tag{4}$$

where v_c is the diffusion rate across the boundary between the intermediate and chemocline layers. The net transport for the chemocline layer is given by:

$$X_c = [-v_c(F_c - F_i) + w_s F_i]/H_c \quad (5)$$

When the mixed layer deepens below the euphotic zone and the intermediate layer vanishes, $H_i = 0$, $F_i = F_m$, and $X_i = 0$ is set. In such conditions, the net flux at the base of the mixed layer is the same as in Eq. (3), except that F_i is replaced by F_c, and Eq. (5) is modified by changing F_i with F_m.

The biological source-sink terms for the phytoplankton, *R(P)*, are as follows:

$$R(P_s) = \phi_{\mathrm{P_s}}\sigma_{P_s}P_s - G_{Z_{mi}}(P_s)Z_{mi} - G_{Z_{me}}(P_s)Z_{me} - G_{N_s}(P_s)N_s - \lambda_{\mathrm{P_s}}\mathrm{P_s} \quad (6)$$

for small phytoplankton,

$$R(P_{da}) = \phi_{\mathrm{P_{da}}}\sigma_{P_{da}}P_{da} - G_{Z_{mi}}(P_{da})Z_{mi} - G_{Z_{me}}(P_{da})Z_{me} - G_{N_s}(P_{da})N_s - \lambda_{\mathrm{P_{da}}}\mathrm{P_{da}} \quad (7)$$

for diatoms,

$$R(P_{di}) = \phi_{\mathrm{P_{di}}}\sigma_{P_{di}}P_{di} - G_{Z_{mi}}(P_{di})Z_{mi} - G_{Z_{me}}(P_{di})Z_{me} - G_{N_s}(P_{di})N_s - \lambda_{\mathrm{P_{di}}}\mathrm{P_{di}} \quad (8)$$

for dinoflagellates,

where ϕ_{P} , σ_P, $G(P)$ and λ_{P} are, respectively, the overall limitation function of the phytoplankton, maximum growth rate of the phytoplankton, grazing exerted on the phytoplankton and natural mortality of the phytoplankton.

The overall limitation function, ϕ_{P}, includes total nitrogen limitation function $\beta_t(N, A) = \left[\frac{A}{R_a+A}\right] + \left[\frac{N}{R_n+N}\right]\exp(-\psi A)$, light limitation function $\alpha(I) = \tanh[\mathrm{aI_s}\exp[-\mathrm{k_w z} - \mathrm{k_c}(\mathrm{P_s} + \mathrm{P_{da}} + \mathrm{P_{di}})]]\,\mathrm{dz}$, and the temperature limitation function $f(T) = Q_{10}^{(T-20)/10}$. R_a is the half saturation constant on ammonium uptake of the phytoplankton, R_n is the half saturation constant on nitrate uptake of the phytoplankton, ψ is the ammonium inhibition on nitrate uptake, a is the photosynthesis efficiency of the phytoplankton, $\mathrm{I_s}$ is the photosynthetically available

radiation, k_w is the light exctinction coefficient and k_c is the self-shading coefficient. The grazing exerted on the phytoplankton is formulated as follows:

$$G_i(P_j) = \sigma_i a_j P_j / (R_j + \sum a_n P_n) \quad (9)$$

where σ_i is the limited growth rate of the consumer, a_j is the food preference of the consumer on the prey and R_i is the half saturation constant of the consumer. This grazing function is also valid for the grazing of gelatinous carnivores on zooplankton.

The biological source-sink terms for the zooplankton, *R(Z)*, are as follows:

$$R(Z_{mi}) = \gamma_{Z_{mi}} G_{Z_{mi}}(P_s) Z_{mi} + \gamma_{Z_{mi}} G_{Z_{mi}}(P_{da}) Z_{mi} + \gamma_{Z_{mi}} G_{Z_{mi}}(P_{di}) Z_{mi} + \gamma_{Z_{mi}} G_{Z_{mi}}(D) Z_{mi} - G_{Z_{me}}(Z_{mi}) Z_{me} - G_{N_s}(Z_{mi}) N_s - G_{Z_a}(Z_{mi}) Z_a - G_{Z_m}(Z_{mi}) Z_m - \mu_{Z_{mi}} Z_{mi} - \lambda_{Z_{mi}} Z_{mi}^2 \quad (10)$$

for microzooplankton,

$$R(Z_{me}) = \gamma_{Z_{me}} G_{Z_{me}}(P_s) Z_{me} + \gamma_{Z_{me}} G_{Z_{me}}(P_{da}) Z_{me} + \gamma_{Z_{me}} G_{Z_{me}}(P_{di}) Z_{me} + \gamma_{Z_{me}} G_{Z_{me}}(Z_{mi}) Z_{me} + \gamma_{Z_{me}} G_{Z_{me}}(N_s) Z_{me} + \gamma_{Z_{me}} G_{Z_{me}}(D) Z_{me} - G_{Z_a}(Z_{me}) Z_a - G_{Z_m}(Z_{me}) Z_m - \mu_{Z_{me}} Z_{me} - \lambda_{Z_{me}} Z_{me}^2 \quad (11)$$

for mesozooplankton,

$$R(Z_a) = \gamma_{Z_a} G_{Z_a}(Z_{mi}) Z_a + \gamma_{Z_a} G_{Z_a}(Z_{me}) Z_a - \mu_{Z_a} Z_a - \lambda_{Z_a} Z_a \quad (12)$$

for *Aurelia aurita*,

$$R(Z_m) = \gamma_{Z_m} G_{Z_m}(Z_{mi}) Z_m + \gamma_{Z_m} G_{Z_m}(Z_{me}) Z_m - \mu_{Z_m} Z_m - \lambda_{Z_m} Z_m \quad (13)$$

for *Mnemiopsis leidyi*.

The terms μ_Z and γ_Z are the excretion rate and assimilation efficiency of zooplankton. The excretion rate and assimilation efficiency are also valid for *Nocliluca scintillans*. The biological source-sink terms for the *Noctiluca scintillans*, *R(N_s)*, are as follows:

$$R(N_s) = \gamma_{N_s} G_{N_s}(P_s) N_s + \gamma_{N_s} G_{N_s}(P_{da}) N_s + \gamma_{N_s} G_{N_s}(P_{di}) N_s + \gamma_{N_s} G_{N_s}(D) N_s + \gamma_{N_s} G_{N_s}(Z_{mi}) N_s - G_{Z_{me}}(N_s) Z_{me} - \mu_{N_s} N_s - \lambda_{\mathrm{N_s}} \mathrm{N_s} \quad (14)$$

for *Noctiluca scintillans*.

The corresponding biological source-sink terms for the labile pelagic detritus *R(D)*, ammonium *R(A)* and nitrate *R(N)* are given by:

$$R(D) = (1 - \gamma_{Z_{mi}})[G_{Z_{mi}}(P_s) Z_{mi} + G_{Z_{mi}}(P_{da}) Z_{mi} + G_{Z_{mi}}(P_{di}) Z_{mi} + G_{Z_{mi}}(D) Z_{mi}] + \left(1 - \gamma_{Z_{me}}\right)[G_{Z_{me}}(P_s) Z_{me} + G_{Z_{me}}(P_{da}) Z_{me} + G_{Z_{me}}(P_{di}) Z_{me} + G_{Z_{me}}(Z_{mi}) Z_{me} + G_{Z_{me}}(N_s) Z_{me} + G_{Z_{me}}(D) Z_{me}] + \left(1 - \gamma_{Z_a}\right)\left[G_{Z_a}(Z_{mi}) Z_a + G_{Z_a}(Z_{me}) Z_a\right] + \left(1 - \gamma_{Z_m}\right)[G_{Z_m}(Z_{mi}) Z_m + G_{Z_m}(Z_{me}) Z_m] + \left(1 - \gamma_{N_s}\right)[G_{N_s}(P_s) N_s + G_{N_s}(P_{da}) N_s + G_{N_s}(P_{di}) N_s + G_{N_s}(D) N_s + G_{N_s}(Z_{mi}) N_s] + \lambda_{\mathrm{P_s}} \mathrm{P_s} + \lambda_{\mathrm{P_{da}}} \mathrm{P_{da}} + \lambda_{\mathrm{P_{di}}} \mathrm{P_{di}} + \lambda_{\mathrm{Z_{mi}}} \mathrm{Z_{mi}^2} + \lambda_{\mathrm{Z_{me}}} \mathrm{Z_{me}^2} + \lambda_{\mathrm{Z_a}} \mathrm{Z_a} + \lambda_{\mathrm{Z_m}} \mathrm{Z_m} + \lambda_{\mathrm{N_s}} \mathrm{N_s} - \gamma_{Z_{mi}} G_{Z_{mi}}(D) Z_{mi} - \gamma_{Z_{me}} G_{Z_{me}}(D) Z_{me} - \gamma_{N_s} G_{N_s}(D) N_s - \varepsilon D \quad (15)$$

$$R(A) = \mu_{Z_{mi}} Z_{mi} + \mu_{Z_{me}} Z_{me} + \mu_{Z_a} Z_a + \mu_{Z_m} Z_m + \mu_{N_s} N_s + \varepsilon D - \Omega_a A - \left(\left[\frac{A}{R_{aP_s} + A}\right]\right) \alpha(I) f(T) \sigma_{P_s} P_s - \left(\left[\frac{A}{R_{aP_{da}} + A}\right]\right) \alpha(I) f(T) \sigma_{P_{da}} P_{da} - \left(\left[\frac{A}{R_{aP_{di}} + A}\right]\right) \alpha(I) f(T) \sigma_{P_{di}} P_{di} \quad (16)$$

$$R(N) = \Omega_a A - \left(\left[\frac{N}{R_{nP_s} + N}\right] \exp(-\psi A)\right) \alpha(I) f(T) \sigma_{P_s} P_s - \left(\left[\frac{N}{R_{nP_{da}} + N}\right] \exp(-\psi A)\right) \alpha(I) f(T) \sigma_{P_{da}} P_{da} - \left(\left[\frac{N}{R_{nP_{di}} + N}\right] \exp(-\psi A)\right) \alpha(I) f(T) \sigma_{P_{di}} P_{di} \quad (17)$$

where ε and Ω_a are the detritus decomposition rate and ammonium oxidation rate respectively.

2.4 Numerical Procedure and Initial Conditions

The equations in the model are forwarded in time using the second order accurate leap-frog iteration scheme. Its instability is controlled by smoothing at every time step using Aselin filter. The equations solved separately for each layer. A time step of 10 minutes is used between the calculations. The model is integrated for 10 years for each simulation in order to reach the equilibrium state. In most of the simulations, the model reached the equilibrium state in first 4 years.

Nitrate concentrations of 0.1 and 1.0 mmol N m^{-3} is set for the mixed and intermediate layers, respectively. In order to represent the subsurface nitrogen pool, nitrate concentration of 3 mmol N m^{-3} is set in the chemocline layer. The initial thickness of mixed and intermediate layers set to 20 m each. The thickness of chemocline layer is set as 60 m.

2.5 Reference Parameter Setting

The parameter setting used for the reference simulation is similar to that given by Oguz et al. (2001b). However, some significant changes have been done in order to obtain a more representative annual cycle of the model compartments. The aim of the model used in Oguz et al. (2001b) was to simulate the seasonal cycle of phytoplankton, seasonal cycle of the other model compartments needed to be improved in order to represent the observations better.

The changed parameters are; self-shading coefficient (Table 1), maximum growth rates of all the compartments, mortality rates of all the compartments except mesozooplankton, excretion rates of zooplankton groups, assimilation efficiencies of gelatinous species, Q_{10} parameters of all the model compartments and half-saturation constants of all model compartments (Table 2).

Food preficiencies of the predators in the model, are the ratios, which sum up to 1 for each predator (Table 3).

Table 1. Parameters of the biological model used in the simulations.

Parameter	Definition	Value
a	Photosynthesis efficiency parameter	0.01 $m^2 W^{-1}$
k_w	Light extinction coefficient	0.08 m^2 $mmol^{-1}$
k_c	Self-shading coefficient	0.04 m^{-1}
R_n	Half-saturation constant in nitrate uptake	0.5 mmol m^{-3}
R_a	Half-saturation constant in ammonium uptake	0.2 mmol m^{-3}
ψ	Ammonium inhibition parameter of nitrate uptake	3 m^3 $mmol^{-1}$
ε	Detritus decomposition rate	0.1 per day
Ω_a	Ammonium oxidation rate	0.1 per day
ν_m, ν_c	Diffusion rates	0.08 m per day
Δt	Time step	600 s
Z_{0a}	Background *Aurelia aurita* biomass	0.1 mmol m^{-3}
Z_{0m}	Background *Mnemiopsis leidyi* biomass	0.1 mmol m^{-3}
t_g	Restoring time of the *Aurelia aurita* and *Mnemiopsis leidyi* biomass	10 days

Table 2. Biological source-sink parameters used in the simulations.

Parameter	Definition	P_s	P_{da}	P_{di}	Z_s	Z_l	Z_n	Z_a	Z_m
σ_i	Maximum growth rates	2.5	3.0	2.0	1.0	0.7	0.4	0.4	0.34
λ_i	Mortality rates	0.06	0.04	0.04	0.06	0.04	0.01	0.005	0.005
μ_i	Excretion rates	-	-	-	0.05	0.05	0.02	0.01	0.01
γ_i	Assimilation efficiencies	-	-	-	0.75	0.75	0.7	0.7	0.7
Q_{10}	Q_{10} parameter of temperature limitation	1.9	1.8	1.9	2.1	1.9	2.0	2.0	2.2
R_i	Half-saturation constant	-	-	-	0.3	0.5	0.38	0.5	0.35

Table 3. Food preficiencies of the predators in the model.

Prey	Predator				
	Z_s	Z_l	Z_n	Z_a	Z_m
P_s	0.45	0.12	0.15	-	-
P_{da}	0.20	0.25	0.25	-	-
P_{di}	0.05	0.15	0.10	-	-
Z_s	-	0.20	0.15	0.5	0.7
Z_l	-	-	-	0.5	0.3
Z_n	-	0.03	-	-	-
D	0.30	0.25	0.35	-	-

2.6 Parameter Settings of Simulations

All of the biological source-sink parameters of the model are changed in the parameter sensitivity analysis. Only the parameters which influenced the ecosystem significantly are presented in the results and conclusions section (Table 4).

In the eutrophication simulations, in order to increase the nutrient flux, vertical diffusion of nitrate from the chemocline layer to the intermediate layer was increased. The rest of the parameters in the model kept unchanged.

Changing the entrainment rate represented the effect of cold and warm winters on the ecosystem. This change affected the layer dynamics as well as biomass transportation between layers.

In the analysis of prey-predator interactions, food competition mechanisms tests, grazing pressures of the top-predators on the predators and preys were changed. These changes was obtained by using direct multipliers in the grazing formula of the top-predators against the specific group.

In order to analyse the top-down control exerted by the gelatinous carnivores in the system, the gelatinous carnivores biomass were removed from the system via decreasing the maximum growth rate of gelatinous carnivores to a very low value.

3 RESULTS AND DISCUSSION

3.1 Numerical Simulations

In this section, 6 different simulations of annual Black Sea ecosystem variability is presented. The ecosystem model described in section 2 is first used to establish a reference simulation that provides the basis for comparison with other simulations designed to test model sensitivity to processes and parameters.

The second simulation consist of several tests done in order to determine the parameter sensitivity. Determining the parameter sensitivity is needed to understand the model dynamics and model robustness and used to adjust the poorly known parameter values.

The third simulation aims to represent the eutrophic conditions in the Black Sea. In this simulation, the model sensitivity to change in the nutrient fluxes is investigated.

In the fourth simulation, the effect of climatic changes to the ecosystem and layer dynamics are tested. The response of the model to changes in the winter climate is investigated by changing the entrainment rate.

The fifth and sixth simulations are done to better understand the prey-predator interactions, food competition and top-down control mechanisms in the model.

3.2 Reference Simulation

The reference simulation is assumed to represent the general features of the basin. The environmental time series input to the ecosystem model are described in the following section. This is followed by descriptions of the simulations of the depth-time distribution of the state variables and of the derived quantities obtained from the reference simulation. The parameters used for the reference simulation are given in the Material and Methods section. These parameters are based on Oguz et al.,

1996,1998, 2001a, and 2001b. Some of these parameters are adjusted through a series of sensitivity studies in order to reproduce the observations.

3.2.1 Observations

In this study, a specific data set is used to test how well the model simulates the general pattern of the seasonal changes of the model compartments' biomass after the *Mnemiopsis leidyi* outburst (1990-1992). The data set, except *Noctiluca scintillans* data, is a combination from the data collected by A.S. Mikaelyan, I.N. Sukhanova (IO RAS, P.P. Shirshov Institute of Oceanology, Russian academy of Sciences,), L.V. Georgieva and L.G. Senichkina (IBSS, Institute of Biology of the Southern Seas). The data was collected during the four ecosystem expeditions of IO RAS in 1991-1992 with R/V Gidrobiolog in 1991 and R/V Vityaz in 1991-1992. The data set was published by Shuskina et al. (1998). *Noctiluca scintillans* data is taken from Kovalev et al. (1996) (Fig. 3).

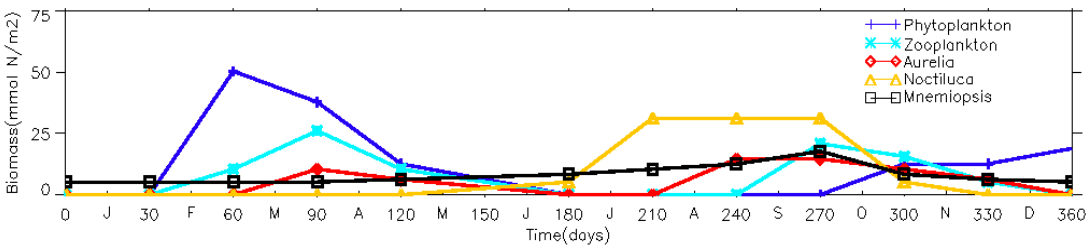

Figure 3. Observed annual biomass distribution of the model compartments. Phytoplankton, zooplankton, *Mnemiopsis leidyi* and *Aurelia aurita* data is taken from Shuskina et al. (1998). *Noctiluca scintillans* data is taken from Kovalev et al. (1996).

The observed annual distributions of the phytoplankton show general features of low biomass during the first 30 days followed by increased biomass from about early-February until late-April, reaching a peak biomass of 50 mmol N m^{-2} and another one that starts around October, reaches a peak biomass of 22 mmol N m^{-2} in December (Fig. 3).

The high zooplankton activity follows the enhanced phytoplankton activity. With a slow development in mid-March, the zooplankton biomass reaches a peak value of 26 mmol N m^{-2} in early-April. The zooplankton biomass decreases slowly and

reaches a minimum of 1 mmol N m^{-2} in late-June and stays constant until September. In September, zooplankton biomass increases up to 22 mmol N m^{-2} in October and decreases slowly in December (Fig. 3).

Noctiluca scintillans biomass has one significant bloom throughout the year. Starting from July, *Noctiluca scintillans* biomass stays on its peak concentration of 30 mmol N m^{-2} until end of October (Fig. 3).

First of the *Aurelia aurita* blooms follows the development of zooplankton in March. This less significant blooms reaches a peak biomass of 10 mmol N m^{-2} and then decreases to its minimum in early-July. At the end of July, *Aurelia aurita* biomass starts developing and its stays at its peak of 20 mmol N m^{-2} until November. In December, *Aurelia aurita* biomass reaches its minimum (Fig. 3).

Mnemiopsis leidyi has a minimum of 5 mmol N m^{-2} throughout the year. Only in summer and autumn months, *Mnemiopsis leidyi* biomass increases. The peak biomass of *Mnemiopsis leidyi* is observed in late-September (Fig. 3).

3.2.2 Reference Simulation Forcing

Wind stress magnitude, total heat flux, photosynthetically available radiation and mixed layer temperature are used in the model as the physical forcings which generate the dynamical changes in the model structure. The daily variations of the physical forcings shown in Figure 4 and Figure 5 are based on basin averaged monthly climatologies (Oguz et al., 2001b).

The magnitude of wind stress and total heat flux affect the entrainment rate and layer dynamics. High wind stress results in higher entrainment rate and deeper mixed layer. The effect of heat flux is similar to the effect of wind stress.

Photosynthetically available radiation (PAR) affects the light limitation function which is affecting the nutrient uptake of phytoplankton groups directly. Mixed layer temperature effects the ecosystem groups directly via temperature limitation function, which hinders or enhances the maximum growth rate.

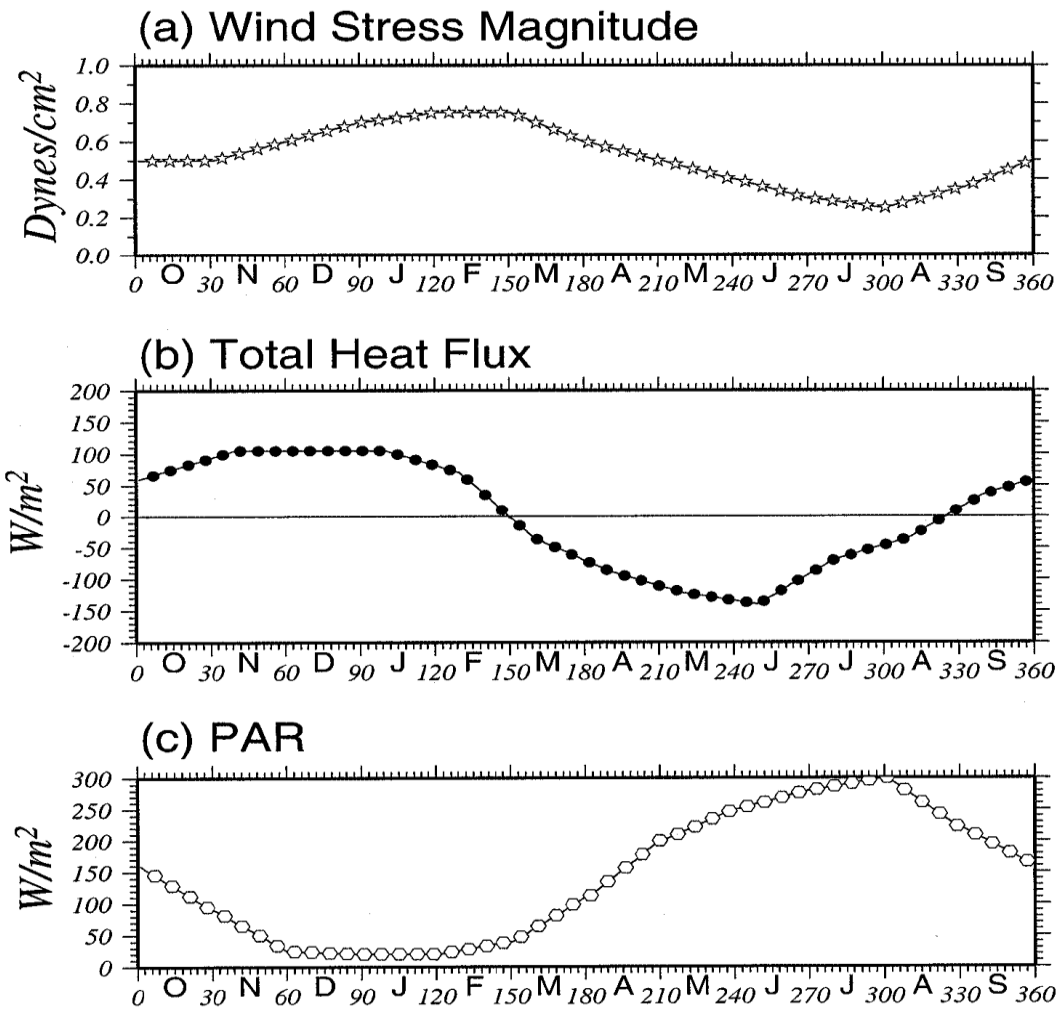

Figure 4. The daily variations of climatological (a) wind stress magnitude, (b) Total heat flux and (c) photosynthetically available radiation (after Oguz et al., (2001b)).

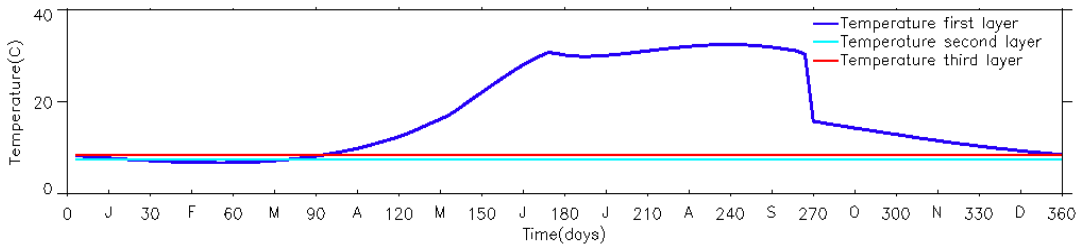

Figure 5. The daily variation of climatological mixed layer temperature.

3.2.3 Simulation of Ecosystem Groups

During the winter months, high nitrate concentrations occur in the mixed layer due to enhanced entrainment. In early-March, the nitrate concentration in the mixed layer reaches its maximum of 100 mmol N m^{-2}. At the end of March, abrupt shallowing in the mixed layer and the euphotic zone occurs (Fig. 6). Thus, all the nitrate accumulates in the third layer. In this period, the maximum concentration of nitrate is achieved (350 mmol N m^{-2}, Fig. 7). Ammonium concentration is very low throughout the year with a maximum of 5 mmol N m^{-2} in the second layer in mid-May (Fig. 8). The reason for low ammonium concentration is the high decomposition rate of ammonium into nitrate.

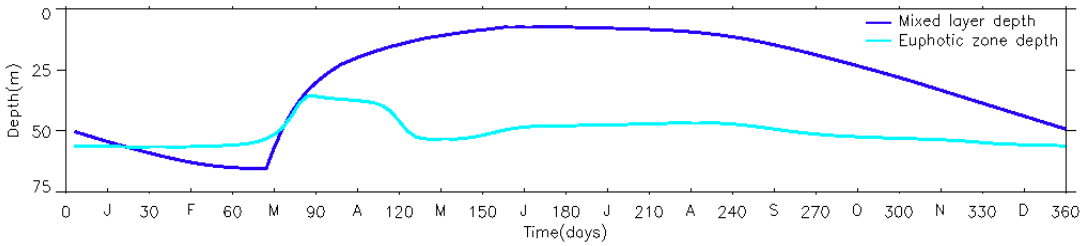

Figure 6. Mixed layer and euphotic zone depths.

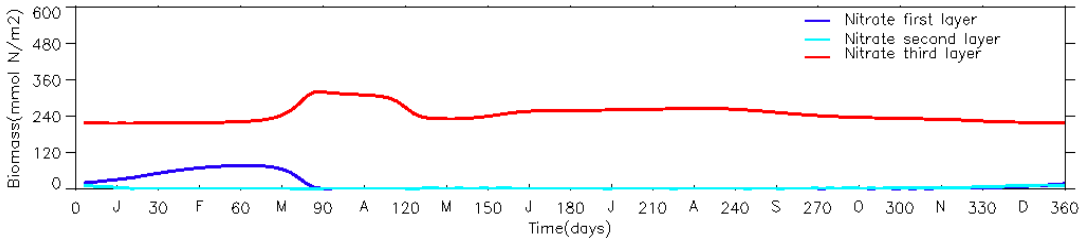

Figure 7. Nitrate concentrations in different layers.

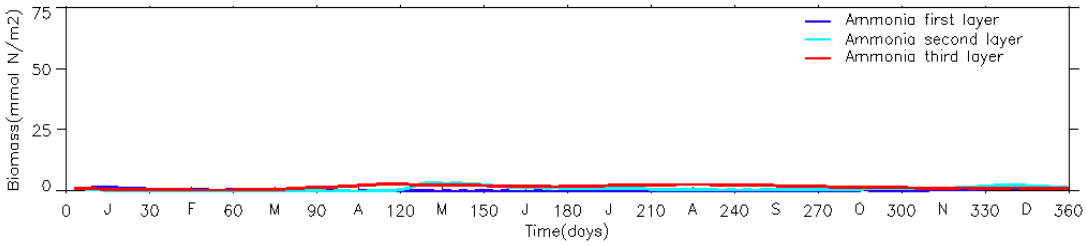

Figure 8. Ammonium concentrations in different layers.

The simulated column integrated annual distributions of the phytoplankton show general features of low biomass during the first 60 days followed by increased

biomass from about early-March until late-April and another one that starts around mid-May (Fig. 9).

The first bloom starts in early-Mach, reaches a peak biomass of 42 mmol N m^{-2} in the mid-March, and declines at the end of April. It corresponds to the end of the winter mixing, where the mixed layer shallows abruptly (Fig. 6). The bloom starts in the mixed layer (Fig. 10), but as the mixed layer shallows, the phytoplankton biomass is observed in the second layer. This is due to regulation of nitrate. Shallowing of the mixed layer causes a decrease in the entrainment rate, which also results in less nutrient transport through the mixed layer, thus low phytoplankton production occurs in the mixed layer. Diatoms being the main group of phytoplankton which constitutes the biomass.

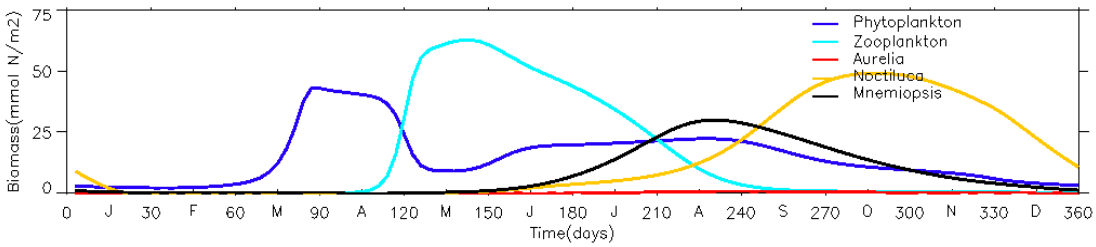

Figure 9. Column integrated biomass of the model compartments.

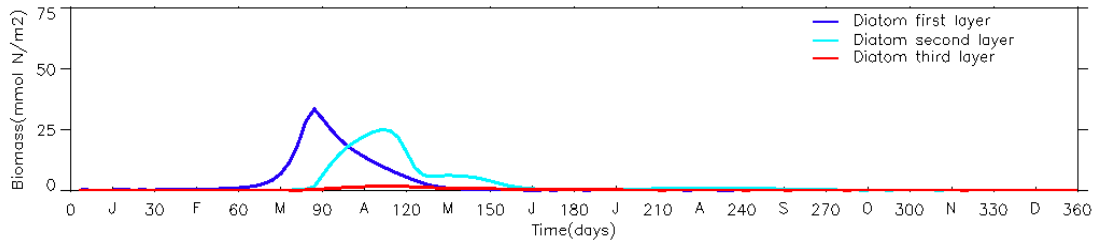

Figure 10. Diatom biomass in different layers.

The second enhanced phytoplankton activity starts in mid-May, reaches its peak biomass of 25 mmol N m^{-2} during early-August. The biomass starts decreasing by mid-August until the end of November, when the total phytoplankton biomass is at a minimum of 5 mmol N m^{-2}. The phytoplankton biomass is observed in the second layer and dinoflagellate is the dominant phytoplankton group (Fig. 11). This enhanced activity is due to decreasing grazing pressure of zooplankton on phytoplankton (mainly dinoflagellates). Small phytoplankton biomass remains very

low throughout the year (Fig. 12), but small phytoplankton group is important in the model, the importance is shown in the parameter sensitivity section.

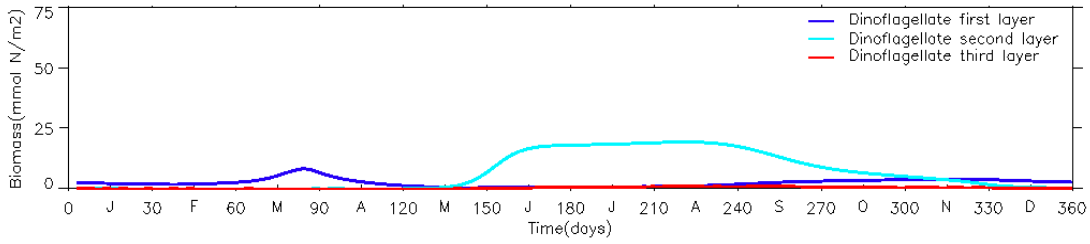

Figure 11. Dinoflagellate biomass in different layers.

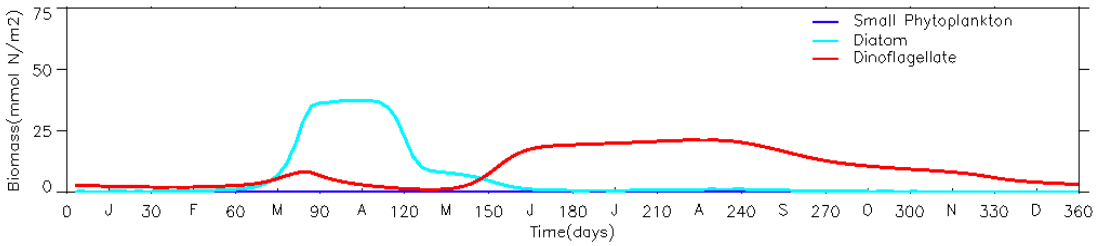

Figure 12. Column integrated biomass of phytoplankton groups.

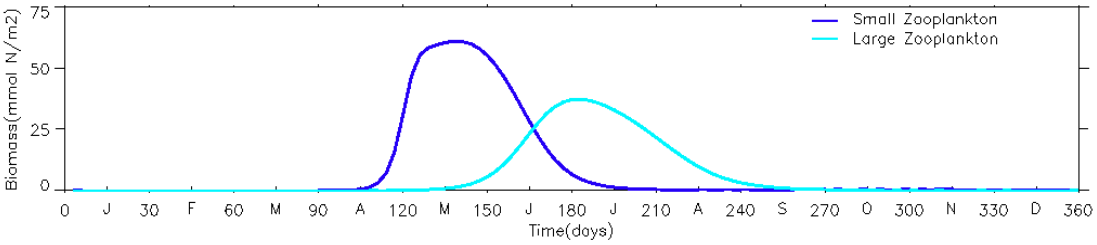

Figure 13. Column integrated biomass of zooplankton groups.

The simulated zooplankton distributions show high temporal variability in both microzooplankton and mesozooplankton biomass concentration (Fig. 9 and Fig. 13). The high zooplankton activity follows the enhanced phytoplankton activity, as a result of prey-predator relationship. With a rapid development in the early-April, the zooplankton biomass reaches a peak value of 60 mmol N m^{-2} in early-May. The zooplankton biomass then decreases slowly and reaches a minimum of 1 mmol N m^{-2} in early-September and stays constant throughout the year. The decrement in the zooplankton biomass is due to high grazing pressure applied by *Mnemiopsis leidyi* and *Aurelia aurita*. Almost all of the zooplankton biomass is in the second layer (Fig. 14), because the prey of zooplankton (phytoplankton) is in the second layer. Microzooplankton is the dominant zooplankton group at the beginning of

zooplankton biomass development. By the end of May, domination shifts to mesozooplankton (Fig. 13).

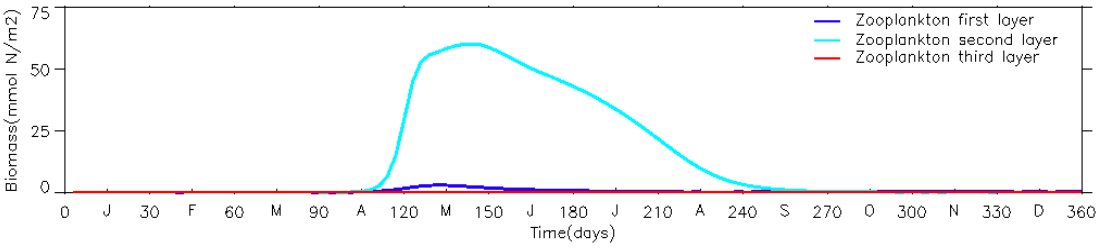

Figure 14. Total zooplankton biomass in different layers.

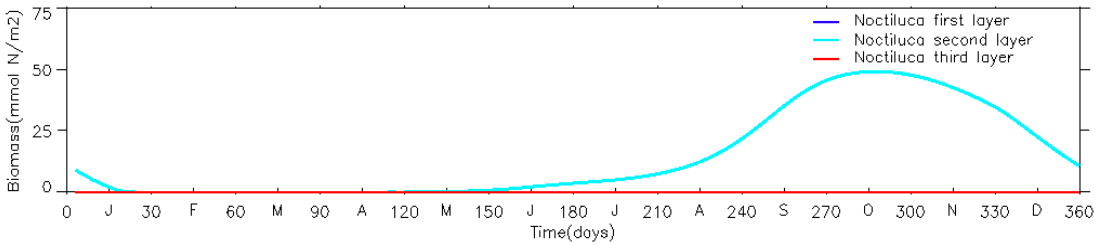

Figure 15. *Noctiluca scintillans* biomass in different layers.

Noctiluca scintillans biomass starts gradually building up in mid-May. In early-August, the biomass development rate increases and the biomass reaches a peak value of 50 mmol N m^{-2} in October. High food availability is the main reason for this increment. The biomass then decreases with an almost constant rate and reaches a minimum biomass of 1 mmol N m^{-2} in mid-January (Fig. 9). All of the biomass is in the second layer, since the food is in the second layer (Fig. 15).

In early-May, *Mnemiopsis leidyi* biomass starts developing gradually, following the high zooplankton activity. The peak biomass of 30 mmol N m^{-2} is obtained in early-August. The biomass then decreases and reaches its minimum of 1 mmol N m^{-2} by the end of December. All of the biomass is in the second layer, because its food zooplankton is abundant in the second layer (Fig. 16).

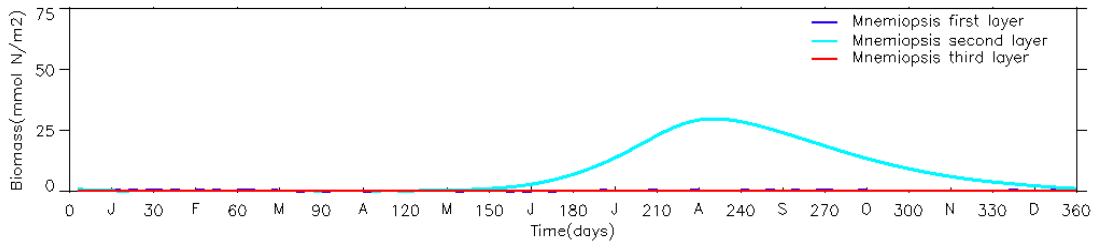

Figure 16. *Mnemiopsis leidyi* biomass in different layers.

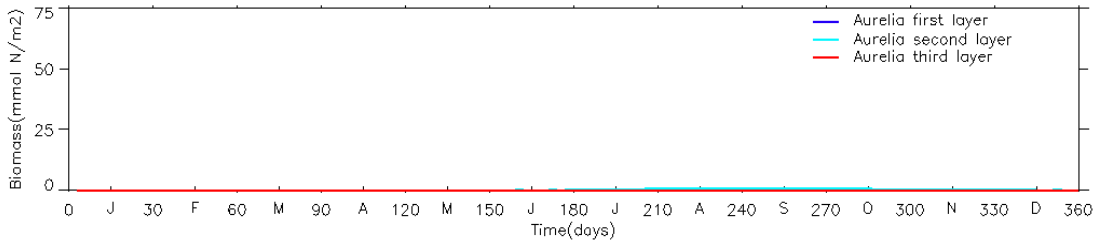

Figure 17. *Aurelia aurita* biomass in different layers.

Aurelia aurita stays at its minimum of 1 mmol N m^{-2} almost throughout the year. Between July and November, biomass of 2 mmol N m^{-2} can be observed (Fig. 9). The low biomass of *Aurelia aurita* is due to the weakness of *Aurelia aurita* in the food competition against *Mnemipsis leidyi* (Mutlu et al., 1994). All of the biomass is in the second layer, because zooplankton is abundant in the second layer (Fig. 17).

Detritus concentration shows a positive correlation to phytoplankton production as expected and thus it is high when the biomass of organisms are high (Fig. 18). Main reasons being the death rate when the biomass of organisms are high and the high predation leading to unassimilated prey biomass (which forms detritus). Detritus reaches its maximum concentration of 10 mmol N m^{-2} is in early-July in the second layer.

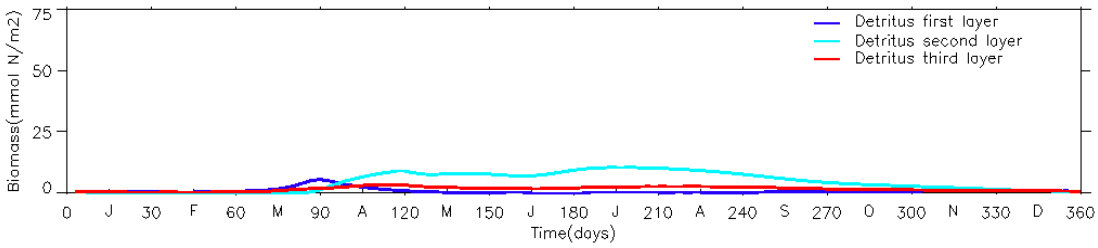

Figure 18. Detritus concentrations in different layers.

In winter months, a deep mixed layer occurs during February to April, the mixed layer depth is at its maximum of 55 m and as a result the second layer disappears. At the beninning of April, abrupt shallowing of the mixed layer and euphotic zone occurs due to the decrement in the entrainment rate and shadowing effect of phytoplankton (Fig. 6). The decrement in the entrainment rate is due to decreasing heat flux (Fig. 4b) and wind stress (Fig. 4a). The euphotic zone gets deeper again as the phytoplankton biomass decreases in early-May and remains almost constant

throughout the year. The mixed layer depth decreases gradually until June, when it reaches its minimum depth of 10 m. At August, the mixed layer gets deeper with an increasing rate as the heat flux and wind stress increases.

The model simulated the spring bloom of phytoplankton with a 1 month shift, however, this shift has no direct effect on the dynamics of the system. Thus, we can say that the spring bloom of phytoplankton is simulated well. The simulated summer bloom of phytoplankton has a higher peak biomass than the observed bloom. This is due to the big shift in *Noctiluca scintillans* bloom. The simulation of *Noctiluca scintillans* bloom is not good. However, this shift didn't affect the system dynamics. Thus, it is acceptable. But the model's simulation for *Noctiluca scintillans* has to be improved.

Instead of two separate blooms of zooplankton as in the observations, the model simulated only one big bloom, which follows the spring bloom of phytoplankton. This successive blooms of phytoplankton and zooplankton shows that the prey-predator relationship between phytoplankton and zooplankton is simulated well in the model. This is more important than simulating the second bloom of zooplankton since the simulations we are going to do with the model are based on trophic interactions.

The simulated bloom of *Mnemiopsis leidyi* fits with the observations. However, the model simulated the annual biomass distribution of *Aurelia aurita* poorly.

3.2.4 Simulated Upper Water Mass Flows

Analyses of the distributions obtained from the reference simulation indicate that microzooplankton grazing on phytoplankton groups (0.463 mmol N m^{-2} d^{-1}) and nitrate uptake by dinoflagellates (1.234 mmol N m^{-2} d^{-1}) provides the primary pathway for mass (i.e. nitrogen) transfer through nutrients to the primary and secondary producers (Fig. 19). Dinoflagellate group of phytoplankton mainly consumes nitrate but low ammonium (annual average of 1.234 mmol N m^{-2} d^{-1} versus 0.318 mmol N m^{-2} d^{-1} respectively). However, diatoms behave differently and they take up as much ammonium as nitrate (0.220 mmol N m^{-2} d^{-1} and 0.290 mmol N m^{-2}

d^{-1} respectively) Nitrogen flow from dinoflagellates through predators (0.814 mmol N m^{-2} d^{-1}) is much higher than through detritus (0.436 mmol N m^{-2} d^{-1}), this is also the case for diatoms (0.299 mmol N m^{-2} d^{-1} through predators, 0.157 mmol N m^{-2} d^{-1} through detritus). Nitrogen flow from and through small phytoplankton is negligible, indicating that small phytoplankton production is also very low.

In the model detritus constitutes the most preferred food for microzooplankton (0.960 mmol N m^{-2} d^{-1}). Whereas, diatoms and dinoflagellates are the secondary preferred food for microzooplankton with much lower nitrogen flow (0.279 mmol N m^{-2} d^{-1} and 0.184 mmol N m^{-2} d^{-1} respectively). Loss of biomass by death and excretion (0.764 mmol N m^{-2} d^{-1} and 0.447 mmol N m^{-2} d^{-1} respectively) is much higher compared to loss of biomass due to predation (0.217 mmol N m^{-2} d^{-1}).

Mesozooplankton mostly feeds on dinoflagellates (0.340 mmol N m^{-2} d^{-1}) and detritus (0.326 mmol N m^{-2} d^{-1}) and microzooplankton (0.190 mmol N m^{-2} d^{-1}) is also a preferred food source. Predation of *Noctiluca scintillans* by mesozooplankton is very low (0.018 mmol N m^{-2} d^{-1}) and mesozooplankton's feeding on diatom is negligible. At the time of high mesozooplankton activity, diatom doesn't exist in the system, because high microzooplankton grazing pressure and also dinoflagellate is stronger in the food competition. Natural death causes the highest loss of biomass (0.344 mmol N m^{-2} d^{-1}) for mesozooplankton. Excretion (0.274 mmol N m^{-2} d^{-1}) and predation by gelatinous carnivores (0.179 mmol N m^{-2} d^{-1}) are the other means of loss of biomass.

Main feeding source for *Noctiluca scintillans* is detritus (0.510 mmol N m^{-2} d^{-1}) and dinoflagellates (0.290 mmol N m^{-2} d^{-1}), diatoms (0.02 mmol N m^{-2} d^{-1}) and microzooplankton (0.008 mmol N m^{-2} d^{-1}) constitute a low share of its diet. Natural death (0.357 mmol N m^{-2} d^{-1}) and excretion (0.179 mmol N m^{-2} d^{-1}) define dominant mechanisms for *Noctiluca scintillans* biomass loss. Loss of biomass via predation by mesozooplankton is very low (0.018 mmol N m^{-2} d^{-1}). This feeding preference of Noctiluca scintillans is consisted with the observations of Elbrachter and Qi, 1998.

Gelatinous carnivores mainly feed on mesozooplankton (0.179 mmol N m^{-2} d^{-1}). Predation of microzooplankton is almost negligible (0.019 mmol N m^{-2} d^{-1}).

Excretion (0.107 mmol N m^{-2} d^{-1}) is the dominant mechanism on loosing biomass while natural death (0.053 mmol N m^{-2} d^{-1}) is the other means of loosing biomass.

Ammonium oxidation to nitrate is moderate (0.313 mmol N m^{-2} d^{-1}). But, detritus decomposition to ammonium is very low (0.027 mmol N m^{-2} d^{-1}).

It is observed that there is an imbalance in nitrate input and output, output is much higher than input. This imbalance occurs since the entrainment and diffusion of nitrate between layers is not shown in Figure 19. There is a continous nitrate supply in the third layer. With a set treshold value, nitrate in the third layer is balanced in every time step.

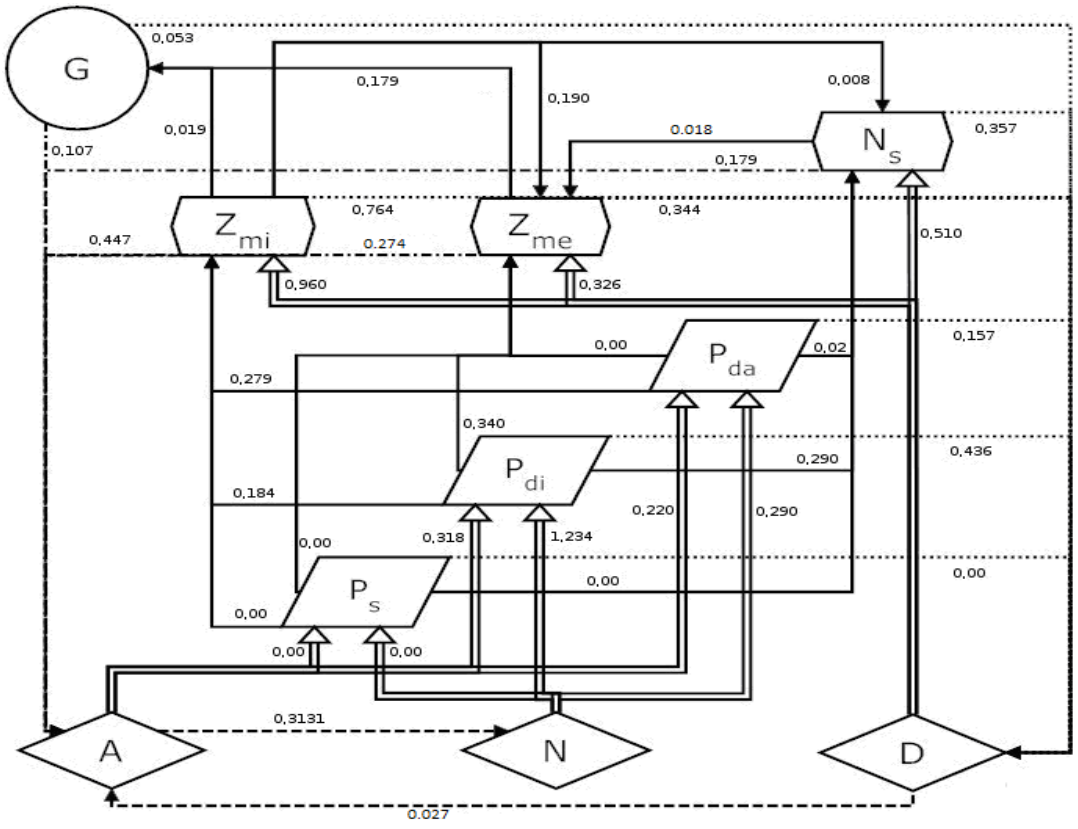

Figure 19. Flowchart of the simulated nitrogen flow (mmol N m^{-2} d^{-1}) obtained for ecosystem model structure used in this study. Arrows indicate the direction of nitrogen transfer between model compartments. The ecosystem variables are annually averaged within the water column (0-100 m). Double lines indicate nutrient and detritus uptake, solid lines indicate predation, dashed lines indicate chemical processes, dotted lines indicate mortality and the dot-dashed lines indicate excretion. Abbreviations on the flow chart are: A- Ammonium, N- Nitrate, D- Detritus, P_s- Small phytoplankton, P_{di}- Dinoflagellates, P_{da}- Diatoms, Z_{mi}- Microzooplankton, Z_{me}- Mesozooplankton, N_s- *Noctiluca scintillans* and G- Gelatinous carnivores.

3.3 Parameter Sensitivity

In this section, sensitivity of the model solutions to variations in maximum growth rates, half saturation constants, assimilation efficiency, mortality and excretion rates was tested. All the parameters have been increased and decreased by 10% and 20%. Because some of the parameters didn't significantly change the model results, only the results of the tests that the model is sensitive are shown in Table 4.

The effects of changing the parameters are shown as percentage change in the annually averaged biomass of total phytoplankton (lowest trophic level), gelatinous carnivores (highest trophic level) and annually averaged total primary production. Some of the important parameters are explained in detail with annual distribution figures.

Table 4. Effect of the sensitive parameters on total phytoplankton biomass, total primary production and gelatinous carnivores biomass.

Changed Group	**Changed Parameter**	**% Change**	**% Change of Total Phytoplankton Biomass**	**% Change of Total Primary Production**	**% Change of Gelatinous Carnivores Biomass**
Small Phytoplankton	Maximum Growth Rate	-20%	+2%	+15%	+27%
Dinoflagellate	Half Saturation Constant in Nitrate Uptake	-20%	+10%	+21%	-23%
	Maximum Growth Rate	+10%	+12%	+17%	-31%
		-10%	-24%	-1%	-45%
Diatom	Half Saturation Constant in Nitrate Uptake	+20%	+16%	+26%	-13%
	Maximum Growth Rate	-20%	+22%	+13%	-47%
	Mortality Rate	+10%	+18%	+22%	-20%
Microzooplankton	Half Saturation Constant	+20%	-12%	+18%	+23%
		-20%	0%	-1%	+31%
	Maximum Growth Rate	+10%	+1%	+2%	+18%
	Excretion Rate	+20%	-8%	+15%	+27%
		-20%	-1%	-6%	+28%
Mesozooplankton	Half Saturation Constant	+10%	+3%	+14%	-38%
		-20%	-6%	+3%	+44%
	Maximum Growth Rate	+10%	-8%	+10%	+51%
		-10%	0%	+12%	-47%
	Excretion Rate	+10%	+7%	+19%	-31%
		-20%	-8%	0%	+40%
Noctiluca scintillans	Half Saturation Constant	+20%	+25%	-2%	+26%
		-10%	-2%	+15%	-35%
	Maximum Growth Rate	+10%	-6%	+17%	-37%
		-10%	+23%	-2%	+27%
	Assimilation	+10%	-4%	+13%	-43%

	Efficiency				
		-20%	+40%	+1%	+26%
	Mortality	-10%	+4%	+16%	-24%
	Excretion	-20%	+2%	+15%	-27%
Aurelia aurita	Half Saturation Constant	-20%	0%	+7%	+20%
	Maximum Growth Rate	+20%	0%	+11%	+25%
	Assimilation Efficiency	+20%	+1%	+4%	+20%
Mnemiopsis leidyi	Half Saturation Constant	+20%	+1%	-1%	+4%
	Maximum Growth Rate	-10%	+4%	+4%	-13%
	Assimilation Efficiency	-20%	-1%	+1%	+14%
	Excretion	+20%	+5%	+5%	+8%

3.3.1 Small Phytoplankton Parameters

A variability of maximum growth rate of small phytoplankton by 20% changed the system significantly. This is important because even though it was shown in the reference simulation section that small phytoplankton biomass is almost zero, variability in small phytoplankton production can affect the system.

Decreasing the maximum growth rate of small phytoplankton increased total primary production, because the nutrient uptake of small phytoplankton decreased and this source is shifted towards other phytoplankton groups which can utilize nutrients better. Total phytoplankton biomass didn't increase as much as total primary production. This is due to the grazing pressure exerted on phytoplankton groups. This grazing pressure increment can be seen from increased gelatinous biomass (Table 4).

Increased total primary production direclty influenced microzooplankton and mesozooplankton and resulted in an increase in their biomass. Because of top-down control of zooplankton groups, together with *Noctiluca scintillans*, the increase in total primary production was not directly reflected to total phytoplankton biomass. High zooplankton biomass yielded to high gelatinous carnivore biomass (Fig. 20).

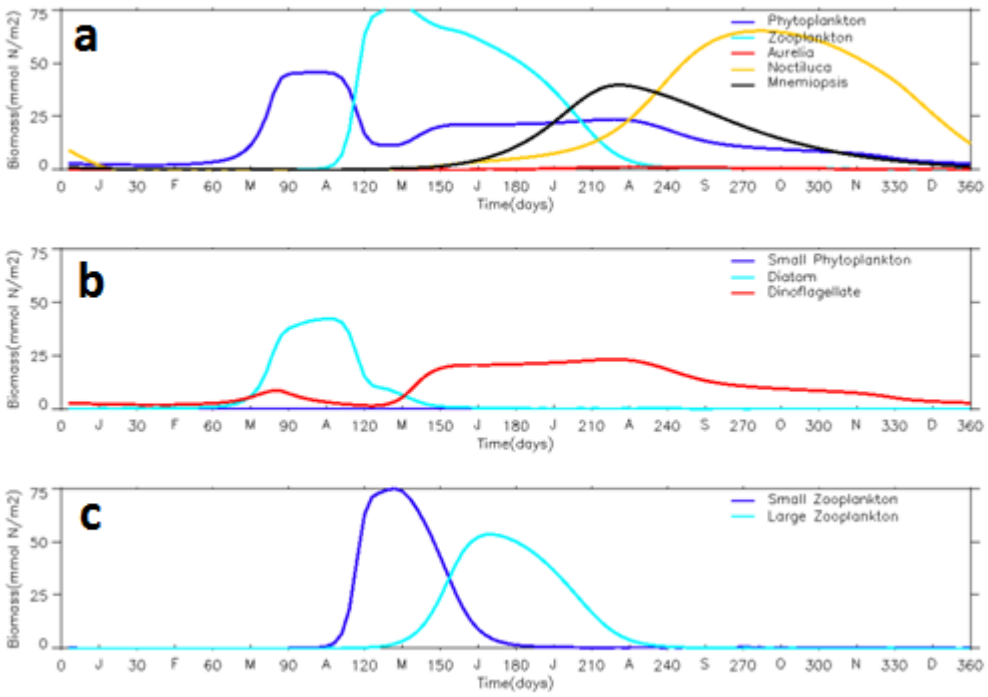

Figure 20. (a) Column integrated biomass of the model compartments,(b) column integrated biomass of phytoplankton groups, (c) column integrated biomass of zooplankton groups with small phytoplankton maximum growth rate decreased by 20%.

3.3.2 Dinoflagellate Parameters

Half-saturation constant in nitrate uptake (decreased by 20%) and maximum growth rate (increased and decreased by 10%) are the main parameters that the dinoflagellate responded.

Decreasing the half-saturation constant in nitrate uptake or increasing the maximum growth rate yielded similar results, because lower half-saturation constant leads to faster growth. Both changes increased the total phytoplankton biomass and total primary production (Table 4). However, this increment in biomass was not reflected to the highest trophic level. This is due to the change in dominant zooplankton (shifted towards mesozooplankton) and gelatinous carnivore type (shifted towards *Aurelia aurita*). This change of domination is a result of strengthening of dinoflagellate in food competition against diatoms. So, first dinoflagellate became the dominant phytoplankton group, this triggered mesozooplankton to be very

dominant for a long time (4 months) and finally this lead to the dominance of *Aurelia aurita* against *Mnemiopsis leidyi*, since *Aurelia aurita* selectively grazes on mesozooplankton, whereas *Mnemiopsis leidyi* prefers microzooplankton (Fig. 21).

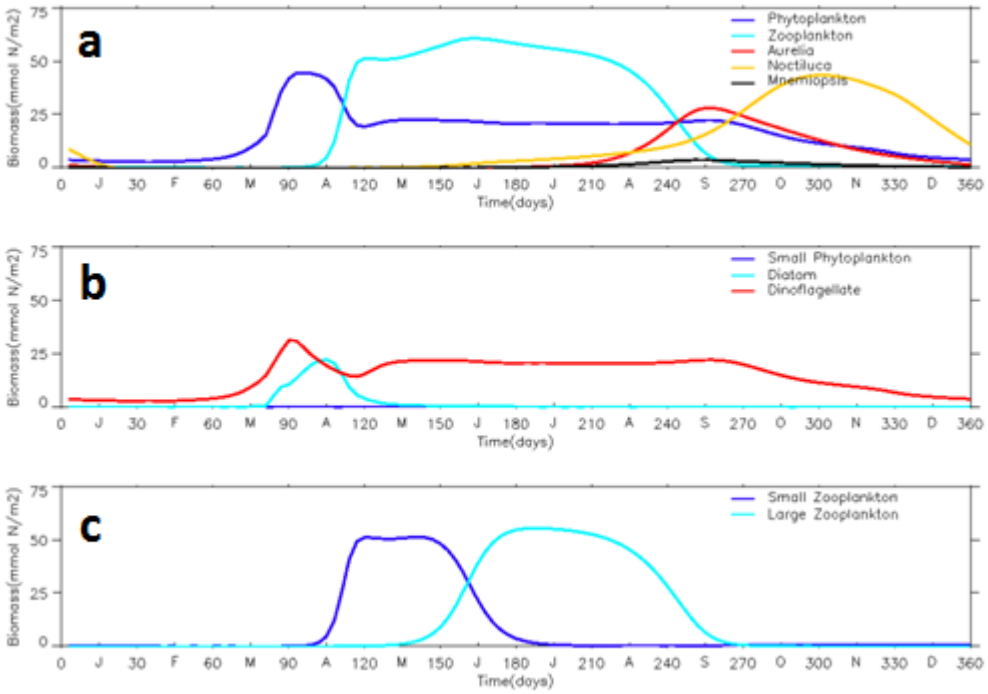

Figure 21. (a) Column integrated biomass of the model compartments,(b) column integrated biomass of phytoplankton groups, (c) column integrated biomass of zooplankton groups with dinoflagellate half saturation concentration in nitrate uptake decreased by 20%.

Decreasing the maximum growth rate resulted in decrement in total phytoplankton biomass, total primary production and biomass of gelatinous carnivores (Table 4). This was expected, because dinoflagellate group is the dominant phytoplankton group, decrement in this dominant group's biomass caused decrement in the biomass of organisms at higher trophic levels which feed on dinoflagellates.

3.3.3 Diatom Parameters

Sensitive parameters of diatoms are; half-saturation constant in nitrate uptake (increased by 20%), maximum growth rate (decreased by 20%) and mortality rate

(increased by 10%). All of these changes are resulted in a similar way in the model. These changes decreased diatom biomass, thus, increased dinoflagellate biomass via weakening the food competition in between. Total phytoplankton biomass and primary production increased, because dinoflagellate took up nutrients more efficiently.

However, increased biomass of total phytoplankton was not transported to the highest trophic level. This is due to the change in dominant zooplankton (shifted towards mesozooplankton) and gelatinous carnivore type (shifted towards *Aurelia aurita*). This change of domination is a result of strengthening of dinoflagellate in food competition against diatoms. So, first dinoflagellate became the dominant phytoplankton group, this triggered mesozooplankton to be very dominant for a long time (4 months) and finally this lead to the dominance of *Aurelia aurita* against *Mnemiopsis leidyi*, since *Aurelia aurita* selectively grazes on mesozooplankton, whereas *Mnemiopsis leidyi* prefers microzooplankton (Fig. 22).

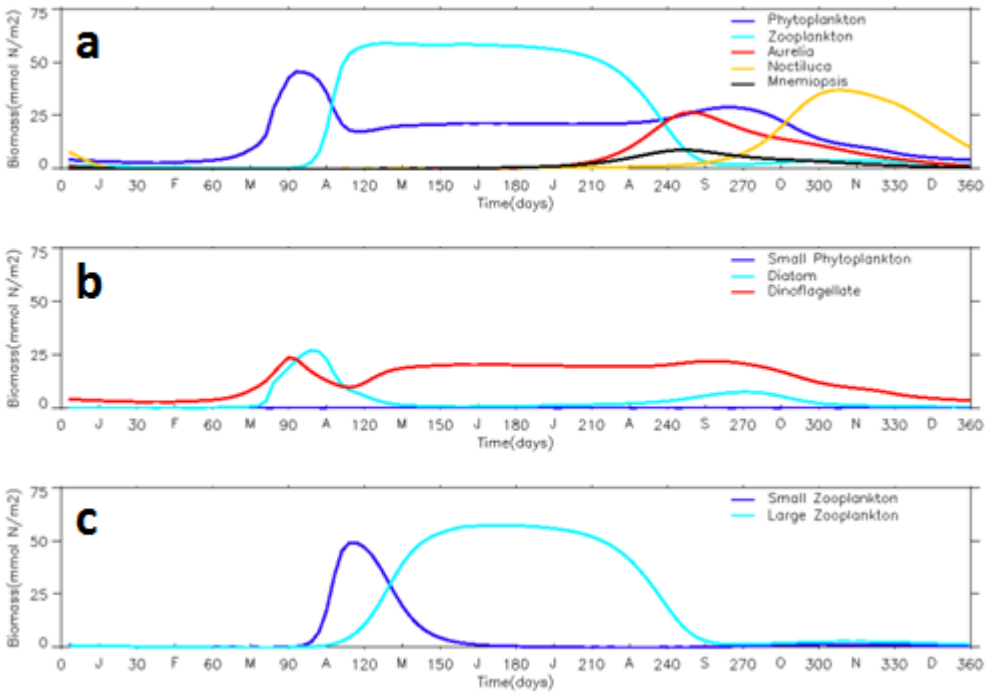

Figure 22. (a) Column integrated biomass of the model compartments,(b) column integrated biomass of phytoplankton groups, (c) column integrated biomass of zooplankton groups with diatom half saturation concentration in nitrate uptake increased by 20%.

3.3.4 Microzooplankton Parameters

Half-saturation constant (increased and decreased by 20%), maximum growth rate (increased by 10%) and excretion rate (increased and decreased by 20%) are the main parameters of microzooplankton, that the model responded.
Increasing the half-saturation constant or excretion rate yielded to similar results. Both changes on parameters resulted in a decrement of total phytoplankton biomass, increment in total primary production and increment in gelatinous carnivores biomass (Table 4). The reason for the decrement in total phytoplankton is because these changes decreased microzooplankton biomass, thus mesozooplankton became the dominant predator on phytoplankton groups (Fig. 23). Gelatinous carnivores biomass increased because they feed on enhanced mesozooplankton biomass.

The decrement of half-saturation constant or excretion rate also yielded to similar results. Both changes on parameters resulted in no significant change of total phytoplankton biomass and total primary production, which is due to controling grazing pressure of microzooplankton, and increased gelatinous carnivores biomass (Table 4). The increment in gelatinous carnivores biomass is due to the increment in microzooplankton biomass (Fig. 24).

Increasing the maximum growth rate didn’t influence total phytoplankton biomass and total primary production significantly, but, resulted in an increment on gelatinous carnivores biomass. This is due to increment on mesozooplankton, prey of gelatinous carnivores.

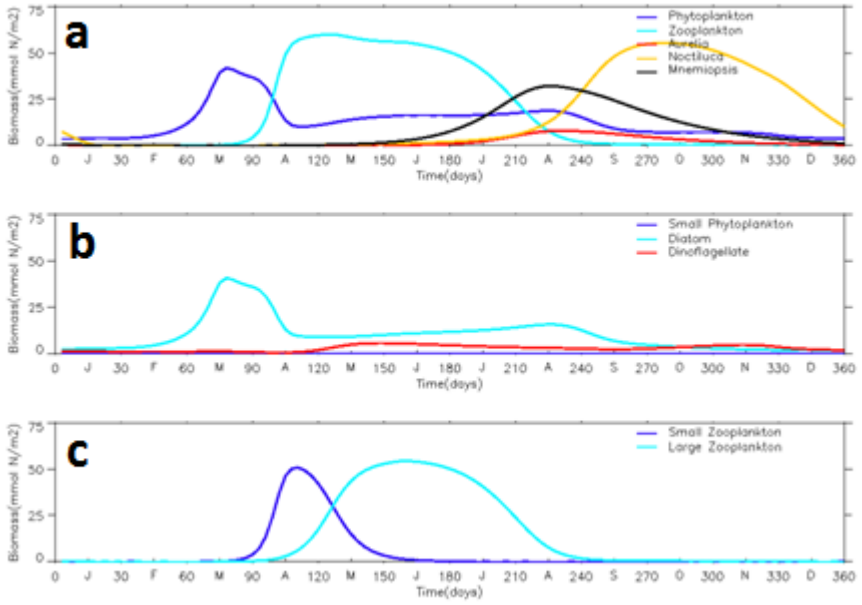

Figure 23. (a) Column integrated biomass of the model compartments,(b) column integrated biomass of phytoplankton groups, (c) column integrated biomass of zooplankton groups with microzooplankton half saturation concentration increased by 20%.

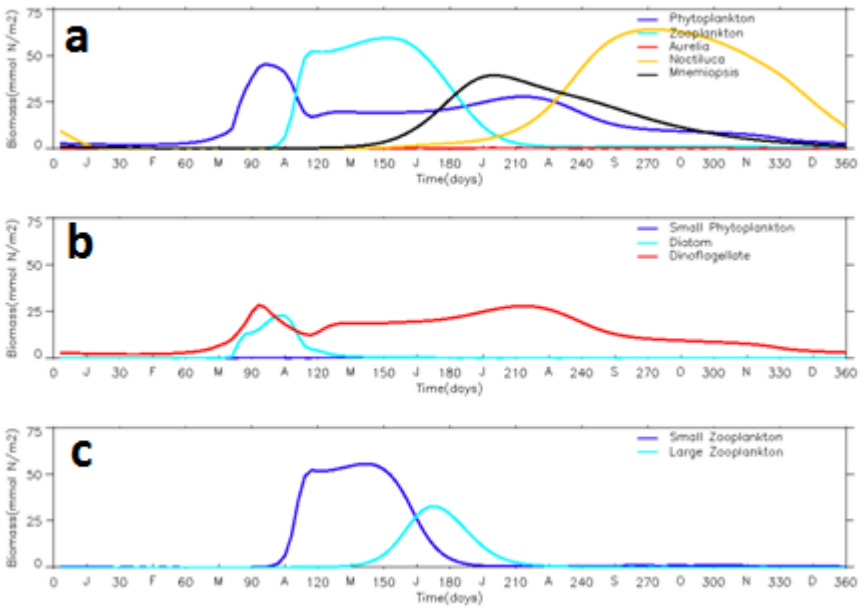

Figure 24. (a) Column integrated biomass of the model compartments,(b) column integrated biomass of phytoplankton groups, (c) column integrated biomass of zooplankton groups with microzooplankton half saturation concentration decreased by 20%.

3.3.5 Mesozooplankton Parameters

Sensitive parameters of mesozooplankton are half-saturation constant (increased by 10% and decreased by 20%), maximum growth rate (increased and decreased by 10%) and excretion rate (increased by 10% and decreased by 20%).

Increasing the half-saturation constant slows down the growth, thus, results in as decrement of maximum growth rate or increment of excretion rate. These changes on parameters resulted in increased total primary production and phytoplankton biomass, because the grazing pressure on phytoplankton exerted by mesozooplankton decreased. Since mesozooplankton biomass decreased, its predator gelatinous carnivores biomass also decreased (Table 4, Fig. 25).

Decreasing half-saturation constant increases the speed of growth. Such a decrement results in better growth as increasing the maximum growth rate. Both changes on parameters increased the mesozooplankton biomass, as decreasing the excretion rate. These three changes have similar effects on the system; higher grazing pressure exerted on phytoplankton by mesozooplankton decreased the total phytoplankton biomass and higher mesozooplankton biomass increased the biomass of its predator, gelatinous carnivores (Table 4).

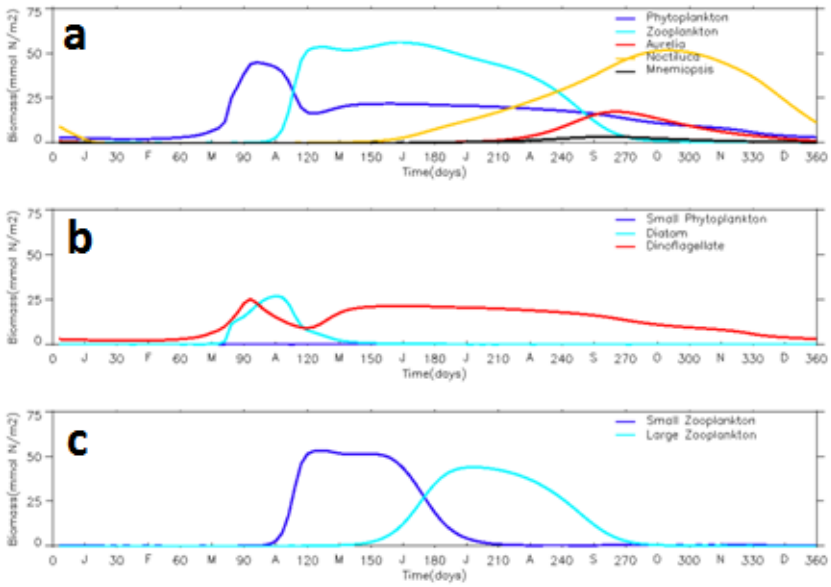

Figure 25. (a) Column integrated biomass of the model compartments,(b) column integrated biomass of phytoplankton groups, (c) column integrated biomass of zooplankton groups with mesozooplankton maximum growth rate decreased by 10%.

3.3.6 Noctiluca scintillans Parameters

Half-saturation constant (increased by 20% and decreased by 10%), maximum growth rate (increased and decreased by 10%), food assimilation efficiency (increased by 10% and decreased by 20%), mortality rate (decreased by 10%) and excretion rate (decreased by 20%) are the main parameters of *Noctiluca scintillans*, that the model responded.

Increasing the food assimilation efficiency affects the system as increasing the maximum growth rate or decreasing the half-saturation constant, because it increases the biomass obtained from the prey. Decreasing the mortality or excretion rates resulted in increased *Noctiluca scintillans* biomass. These changes of parameters decreased the total phytoplankton biomass slightly and increased the total primary production significantly (Table 4). The reason for the increment in total primary production is, increased dinoflagellate production due to weakened food competition between the phytoplankton groups, thus domination of dinoflagellate (Fig. 26). The reason of decreased total phytoplankton biomass is the increased grazing pressure

exerted by increased *Noctiluca scintillans* biomass. High *Noctiluca scintillans* biomass in 6 months of the year inhibited microzooplankton and mesozooplankton to feed on total phytoplankton much (via food competition), thus, decreasing the food of gelatinous carnivores, which resulted in decreased gelatinous carnivores biomass (Fig. 26).

Increased half-saturation constant, decreased maximum growth rate or assimilation efficiency decreased the grazing pressure exerted by *Noctiluca scintillans* on total phytoplankton, also shifted the *Noctiluca scintillans* bloom in winter one month later (Fig. 27). In this gap, zooplankton groups produced and grazed by *Mnemiopsis leidyi*, thus gelatinous carnivores biomass increased. Low grazing pressure exerted on phytoplankton groups increased the total phytoplankton biomass (Table 4, Fig. 27).

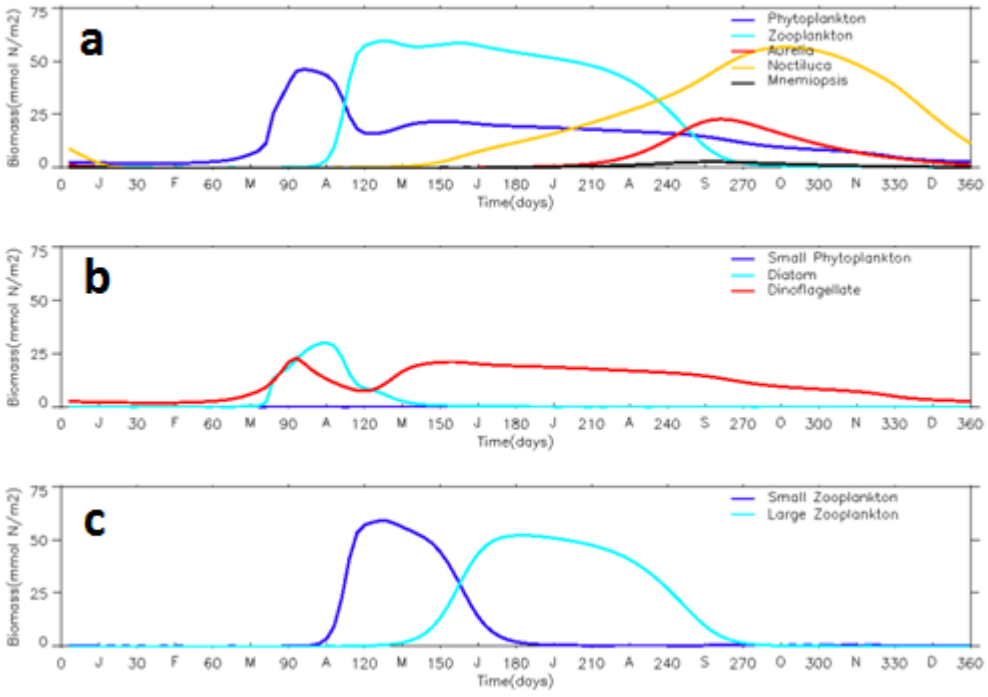

Figure 26. (a) Column integrated biomass of the model compartments,(b) column integrated biomass of phytoplankton groups, (c) column integrated biomass of zooplankton groups with *Noctiluca scintillans* maximum growth rate increased by 10%.

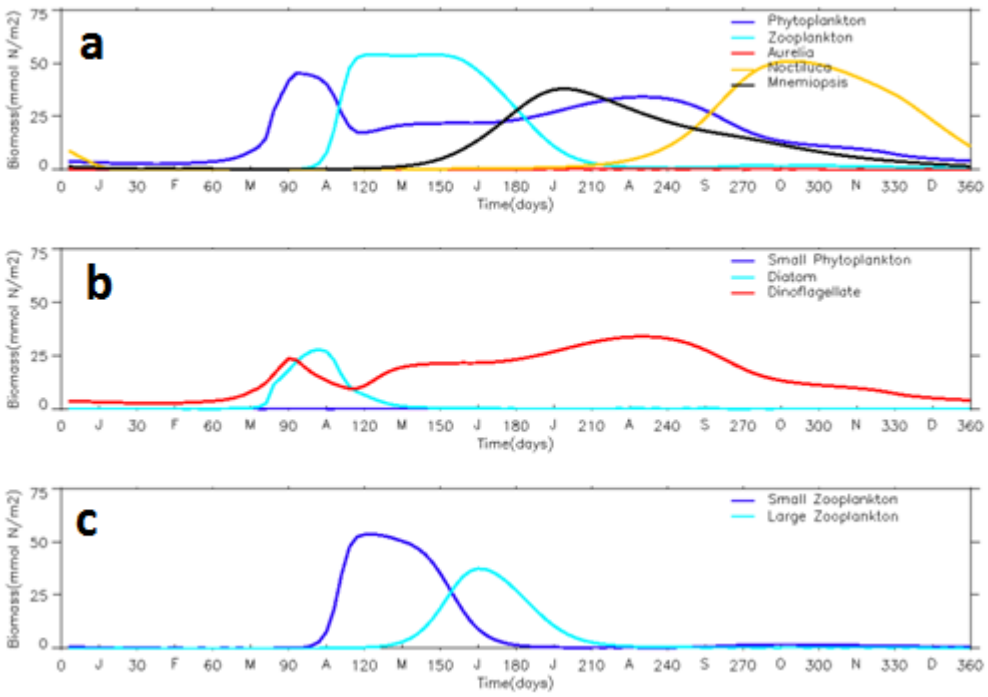

Figure 27. (a) Column integrated biomass of the model compartments,(b) column integrated biomass of phytoplankton groups, (c) column integrated biomass of zooplankton groups with *Noctiluca scintillans* maximum growth rate decreased by 10%.

3.3.7 Aurelia aurita Parameters

Half-saturation constant (decreased by 20%), maximum growth rate (increased by 20%) and assimilation efficiency (increased by 20%) are the main parameters of *Aurelia aurita*, that the model responded.

These changes of parameters all resulted in similar, increased total primary production and gelatinous carnivores biomass (Table 4). Increased grazing pressure on zooplankton groups by *Aurelia aurita* caused higher nutrient recycle (since there are more dead biomass to be recycled), thus increased the total primary production. The changes of parameters didn't influence total phytoplankton significantly, the reason for this is the increased grazing of enhanced microzooplankton (because *Aurelia aurita* prefers consuming microzooplankton less than *Mnemiopsis leidyi* does) on total phytoplankton.

3.3.8 Mnemiopsis leidyi Parameters

Experiments show that the model is most sensitive to variability in half-saturation constant (increased by 20%), maximum growth rate (decreased by 10%), assimilation efficiency (decreased by 20%) and excretion rate (increased by 20%) parameters of *Mnemiopsis leidyi*.

As expected, all the parameter changes inhibited *Mnemiopsis leidyi* population and resulted in dominance of *Aureli aurita*. Changes in total phytoplankton biomass and primary production were very small (Table 4). Decrement on maximum growth rate and assimilation efficiency increased *Aurelia aurita* biomass significantly, since these changes in parameters weakened *Mnemiopsis leidyi*'s competitive strength in the food competition against *Aurelia aurita* (Fig. 28). The gelatinous carnivores grazing pressure on zooplankton groups didn't change and so the total phytoplankton biomass and total primary production didn't change.

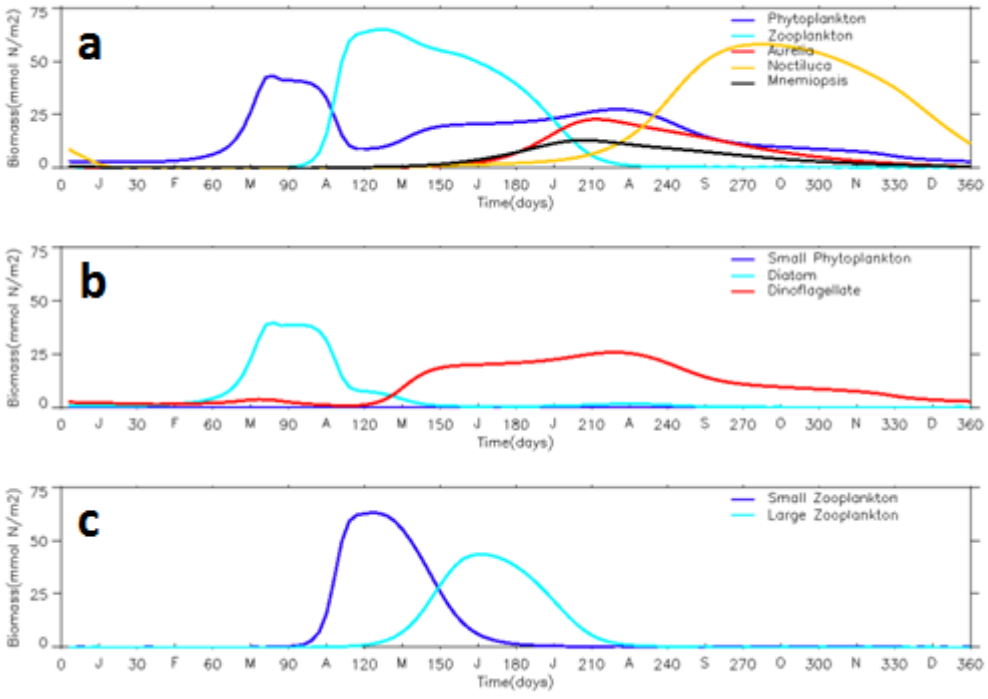

Figure 28. (a) Column integrated biomass of the model compartments,(b) column integrated biomass of phytoplankton groups, (c) column integrated biomass of zooplankton groups with *Mnemiopsis leidyi* maximum growth rate decreased by 10%.

3.4 Eutrophication Simulations

In this section, effect of eutrophication on the model ecosystem has been tested by increasing the nitrate flux from the third layer to the upper layers. By changing the nitrate flux, the nitrate concentration in the upper layers increases, thus increasing the productivity of the upper layers.

Two tests are done to investigate the effect of eutrophication. In the first test, nutrient flux increased by 10% and in the second test, nutrient flux increased by 20%. Further increment on nutrient flux disturbs the robustness of the model.

In the first test, the observed annual distributions of the organisms were the same as the reference simulation in the means of bloom timing. However, slight increments on biomass of organisms were observed. Phytoplankton peak biomass increased by 2 mmol N m^{-2}, microzooplankton peak biomass increased by 3 mmol N m^{-2}, mesozooplankton peak biomass increased by 2 mmol N m^{-2}, *Noctiluca scintillans* peak biomass increased by 5 mmol N m^{-2}, *Aurelia aurita* peak biomass increased by 1 mmol N m^{-2} and *Mnemiopsis leidyi* peak biomass increased by 2 mmol N m^{-2} (Fig. 29).

In the second test, the observed annual distributions of the organisms were the same as the reference simulation in the means of bloom timing also. However, slight increments on biomass of organisms were observed. Phytoplankton peak biomass increased by 5 mmol N m^{-2}, microzooplankton peak biomass increased by 7 mmol N m^{-2}, mesozooplankton peak biomass increased by 10 mmol N m^{-2}, *Noctiluca scintillans* peak biomass increased by 25 mmol N m^{-2}, *Aurelia aurita* peak biomass increased by 1 mmol N m^{-2} and *Mnemiopsis leidyi* peak biomass increased by 3 mmol N m^{-2} (Fig. 30).

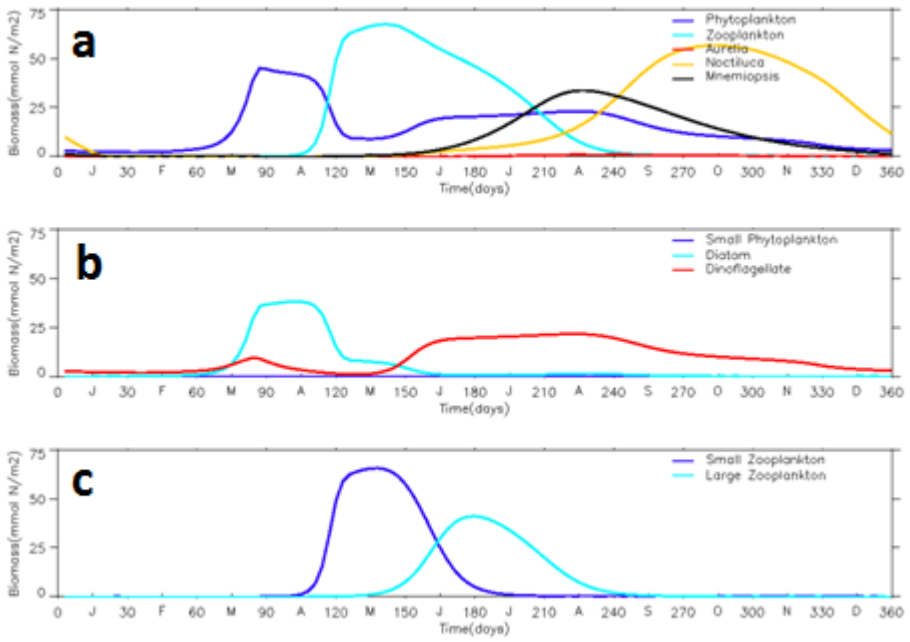

Figure 29. (a) Column integrated biomass of the model compartments,(b) column integrated biomass of phytoplankton groups, (c) column integrated biomass of zooplankton groups with nitrate flux increased by 10%.

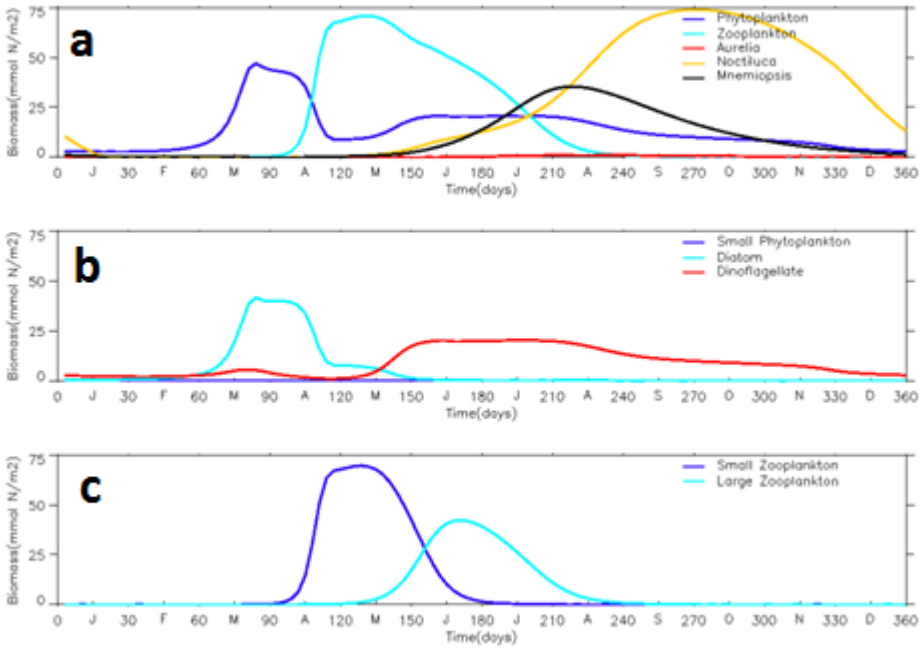

Figure 30. (a) Column integrated biomass of the model compartments,(b) column integrated biomass of phytoplankton groups, (c) column integrated biomass of zooplankton groups with nitrate flux increased by 20%.

In both of the tests, temporal distributions of the model compartments didn't change. Because the overall biomass of the model compartments changed slightly in a way that this changes didn't effect the pre-predator interactions.

The reason for a higher increment on *Noctiluca scintillans* biomass is the strength of *Noctiluca scintillans* in the food competition with zooplankton. The increase in the biomass of the groups is the result of enhanced primary production with increased nutrients. These results are the expected result of eutrophication, as described by Oguz et al. (2009b).

3.5 Cold and Warm Winter Simulations

In this section, effects of the cold and warm winters on the organisms of the system have been tested. It is known that, winter season temperatures can play an important role on how the seasonal dynamics of the Black sea ecosystem may evolve (Oguz, 2005b; Yunev et al., 2007). In the model, the effect of cold and warm winters is tested by modifying the entrainment rate. Entrainment rate controls both physical layer dynamics and mass transportation between layers. By changing the entrainment rate, the feature of the winter thermocline changes. This change in the feature (mainly shifting of the time of the mixed layer shallowing), affects the mass transport (mainly nutrient) between layers, thus affect the productivity of the upper layers.

3.5.1 Warm Winter Simulation

The first simulation is a warm winter simulation. In warm winters, it is expected that the mixed layer will shallow earlier than normal winters. This causes lower nutrient suply from bottom to upper layers, thus lower production in the upper, euphotic zone waters. So, throughout the year, lower biomass of the organisms from different trophic levels is observed. The entrainment rate in this simulation decreased by 10%. It has been observed that the mixed layer started shallowing 5-6 days earlier (Fig. 31). Also, the maximum depth of mixed layer is achieved 10 days later than normal winters (Fig. 31).

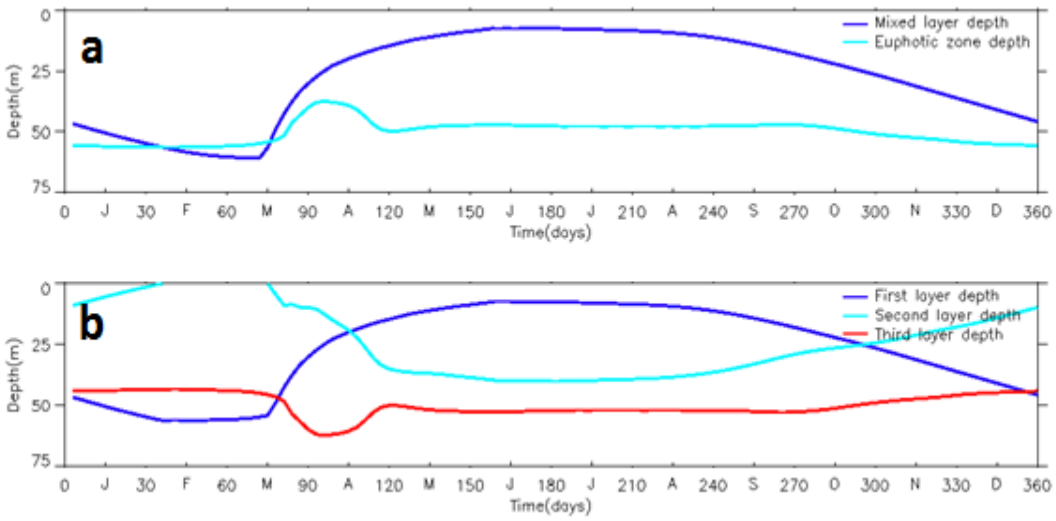

Figure 31. (a) Mixed layer and euphotic zone depths, (b) first, second and third layer depths with entrainment rate decreased by 10%.

The influence of warm winters on the lower trophic levels was minor, however the gelatinous organisms highly influenced by this change.

Spring bloom of phytoplankton didn't shift, but diatom domination was no longer valid. No change in the peak biomass occured, but the phytoplankton biomass started decreasing 10 days earlier. Microzooplankton biomass started developing 10 days earlier with a lower peak in biomass. There is no shift in the biomass decreasing timing of microzooplankton. Mesozooplankton activity starts just as regular, but the peak biomass is higher. Also, the duration of the peak biomass lasts 2 more months, at mid-August mesozooplankton starts to decrease (Fig. 32).

Noctiluca scintillans biomass starts developing timely, but with a smaller rate. The peak biomass shifted for a month and the amount decreased almost 20% (Fig. 32).

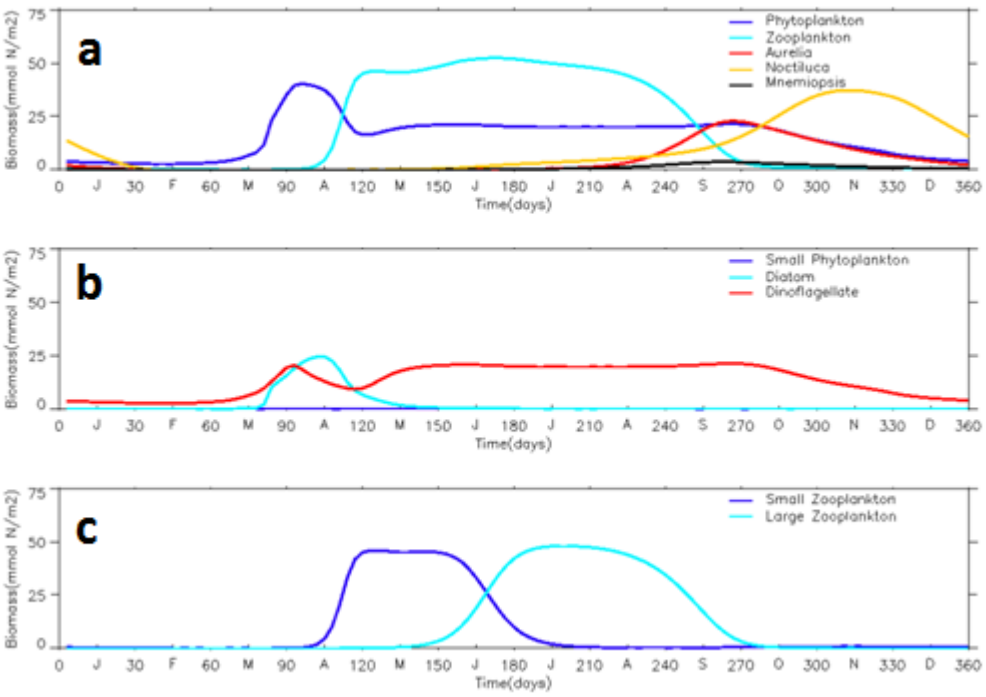

Figure 32. (a) Column integrated biomass of the model compartments,(b) column integrated biomass of phytoplankton groups, (c) column integrated biomass of zooplankton groups with entrainment rate decreased by 10%.

Very high *Aurelia aurita* biomass is observed at early-August with a peak biomass of 25 mmol N m^{-2} in early-October. In mid-January, *Aurelia aurita* biomass decreases to its minimum of about 1 mmol N m^{-2} and is constant until August (Fig. 32). *Mnemiopsis leidyi* biomass starts to develop at the eginning of July with a very low rate and reaches its peak of 4 mmol N m^{-2} in late-September, while it was supposed to reach its peak of 26 mmol N m^{-2} in late-August (Fig. 32). Increase in the biomass of mesozooplankton is the reason of dominancy shift in the gelatinous carnivores towards *Aurelia aurita*; *Aurelia aurita* prefers feeding on mesozooplankton more than *Mnemiopsis leidyi* does.

Oguz (2005b) indicates that, in late 1980s, when the outburst of *Mnemiopsis leidyi* occured in the Black Sea, the winters were warmer. He also suggested that, the warm winters control the timing of *Mnemiopsis leidyi* outburst. However, the model resulted in a decrement of *Mnemiopsis leidyi* biomass in warm winter. The

incompatibility of the model result with observations is due to the lack of temperature effect on *Mnemiopsis leidyi* formula coded in the model.

3.5.2 Cold Winter Simulation

The second simulation is a cold winter simulation. In cold winters, it is expected that the mixed layer will shallow later than normal winters. This causes higher nutrient supply from bottom to upper layers, thus increase production in the upper, euphotic zone waters. So, throughout the year, higher biomass of the organisms from different trophic levels is observed. The entrainment rate in this simulation increased by 20%. It has been observed that the mixed layer started shallowing 10 days later (Fig. 33). Also, the maximum depth of mixed layer achieved 10 days later than normal winters (Fig. 33).

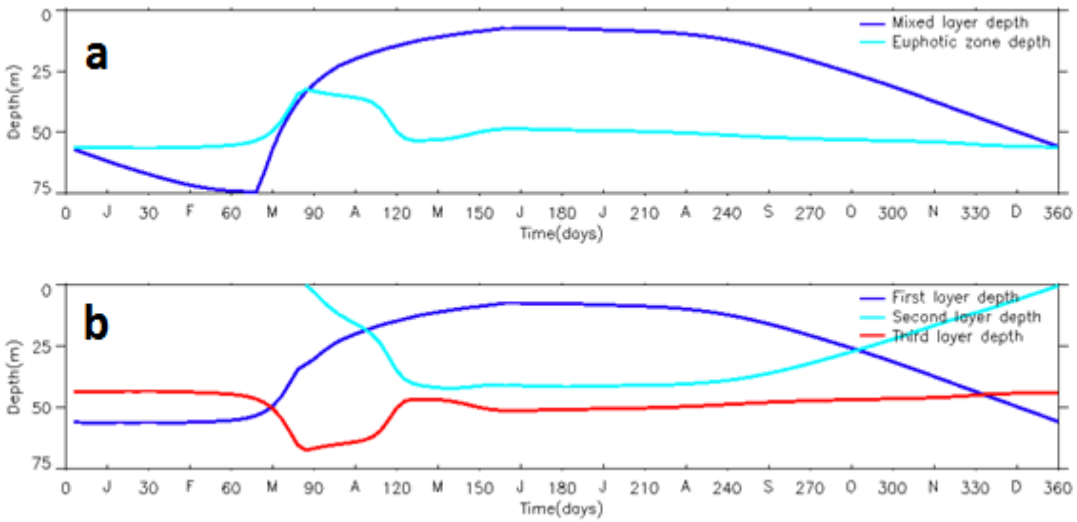

Figure 33. (a) Mixed layer and euphotic zone depths, (b) first, second and third layer depths with entrainment rate increasd by 20%.

The influence of cold winters on the lower trophic levels was minor, however the *Noctiluca scintillans* highly influenced by this change.

Spring bloom of phytoplankton didn't shift, but the peak biomass is increased by 5 mmol N m^{-2}. Microzooplankton peak biomass also increased by 5 mmol N/m^2 due to

prey-predator dynamics. The peak biomass of mesozooplankton didn't change, but the minimum biomass is achieved 10 days later (Fig. 34).

Biomass development of *Noctiluca scintillans* started 1 month earlier and the biomass increased with a high rate. The reason for this shift is the increased primary production. Since *Noctiluca scintillans* is stronger in the food competition against zooplankton, higher primary production increased *Noctiluca scintillans* biomass. The peak biomass of 65 mmol N m^{-2} was observed in late-September (Fig. 34).

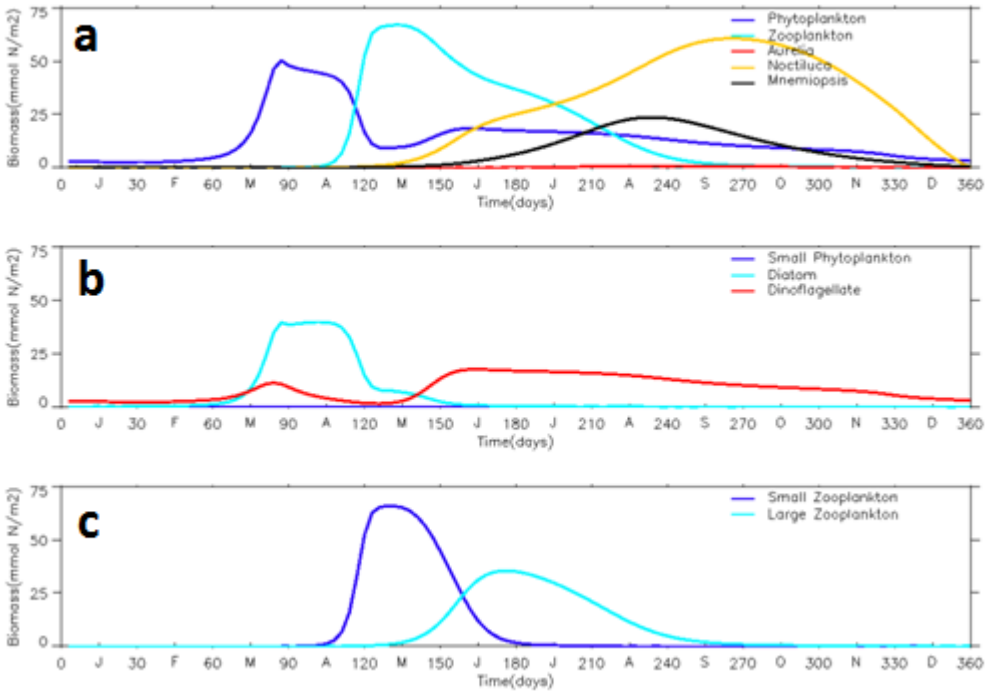

Figure 34. (a) Column integrated biomass of the model compartments,(b) column integrated biomass of phytoplankton groups, (c) column integrated biomass of zooplankton groups with entrainment rate increased by 20%.

The biomass of gelatinous carnivores didn't change significantly (Fig. 34). Because, *Noctiluca scintillans* is stronger in the food competition on increased microzooplankton against gelatinous carnivores. Moreover, the other prey of the gelatinous carnivores didn't change.

Oguz (2005b), Purcell et al. (2001) and Shiganova et al. (2003) pointed out the relation between phytoplankton and *Mnemiopsis leidyi* biomass development and the cold winters. They identified an enhanced phytoplankton biomass in cold winters, and a decreased *Mnemiopsis leidyi* development. The model simulated the increment in phytoplankton biomass well. However, the reduction in the *Mnemiopsis leidyi* biomass couldn't be simulated.

3.6 Prey-Predator Interactions, Food Competition and Top-down Control Mechanisms

In this section, the prey-predator, food competition and top-down control exerted by the gelatinous carnivores mechanisms are analysed in detail using a series of simulations. The prey-predator and food competition mechanisms are combined in guild-like systems in which, a top-predator is feeding on both a consumer and its prey. This mechanism is called the intraguild predation theory (IGP, Holt and Polis, 1996; Polis et al., 1989).

Two main cases of intraguild predation mechanisms occur in the model. These cases are:

a. Mesozooplankton feeds on both microzooplankton and phytoplankton groups, whereas microzooplankton is feeding on phytoplankton groups. In this mechanism, both prey-predator and competition relationships occur between mesozooplankton and microzooplankton.

b. Gelatinous carnivores feed on both mesozooplankton and microzooplankton, whereas mesozooplankton is feeding on microzooplankton. In this mechanism, both prey-predator and competition relationships occur between gelatinous carnivores and mesozooplankton.

The top-down control mechanism is the regulation of the lowest trophic level organisms by the top predators via cascading across multiple trophic levels (Oguz et al., 2001a, Hairston et al., 1960).

These mechanisms are analysed by changing food preferences of the top predator in the guild system, and eliminating *Aurelia aurita* and *Mnemiopsis leidyi* from the system.

3.6.1 Test 1: Gelatinous carnivores, mesozooplankton and microzooplankton guild

In test 1, the intraguild system where gelatinous carnivores act as the top predator, mesozooplankton acts as the consumer and microzooplankton acts as the prey is analysed. In the first two simulations, grazing pressure of gelatinous carnivores on mesozooplankton is reduced. This reduction has weakened the prey-predator relation between gelatinous carnivores and mesozooplankton, thus, food competition became stronger. Results showed that, when the grazing pressure is reduced by 10% and 40%, biomass of gelatinous carnivores and mesozooplankton increased, biomass of microzooplankton decreased (Table 5). The increment in mesozooplankton is due to reduced grazing pressure, and this increment decreased microzooplankton biomass via prey-predator interaction. The reduction of grazing pressure on mesozooplankton, on the long term, increased the biomass of gelatinous carnivores, while a decrement was expected. The reason for this increment can be explained in terms of mesozooplankton biomass increase for two reasons; one is the reduced exerted grazing pressure, the other reason is higher grazing of mesozooplankton on microzooplankton due to increased mesozooplankton biomass. The biomass increment of mesozooplankton, due to increased microzooplankton grazing of mesozooplankton, causes an increase in gelatinous carnivores biomass.

In the last simulation, grazing pressure of gelatinous carnivores on microzooplankton is reduced. This reduction has weakened the food competition between gelatinous carnivores and mesozooplankton, thus, prey-predator interaction became stronger. Results showed that, when the grazing pressure of gelatinous carnivores on microzooplankton is reduced by 50%, gelatinous carnivores biomass and mesozooplankton biomass increased, microzooplankton biomass decreased (Table 5). Another important result is that, the dominancy of *Mnemiopsis leidyi* in the gelatinous carnivores shifted to the dominancy of *Aurelia aurita*, thus, the equal food preference on mesozooplankton and microzooplankton changed to higher food

preference on mesozooplankton (Fig. 35). The decreased grazing pressure on microzooplankton by the gelatinous carnivores enhanced the microzooplankton production, which led to an increment in mesozooplankton biomass. Increment of mesozooplankton biomass, however, on the long term increased the grazing pressure exerted by mesozooplankton on microzooplankton, thus, decreased the microzooplankton biomass.

Table 5. Annually averaged gelatinous carnivores, mesozooplankton and microzooplankton biomass with different gelatinous carnivores grazing preferencies (mmol N m^{-2} day^{-1}).

Simulation	**Gelatinous carnivores biomass**	**Mesozooplankton biomass**	**Microzooplankton biomass**
Reference	7,93	5,67	7,79
Gelatinous carnivores grazing on mesozooplankton is reduced by 10%	9,59	6,79	7,42
Gelatinous carnivores grazing on mesozooplankton is reduced by 40%	11,41	14,94	4,99
Gelatinous carnivores grazing on microzooplankton is reduced by 50%	8,08	8,19	6,84

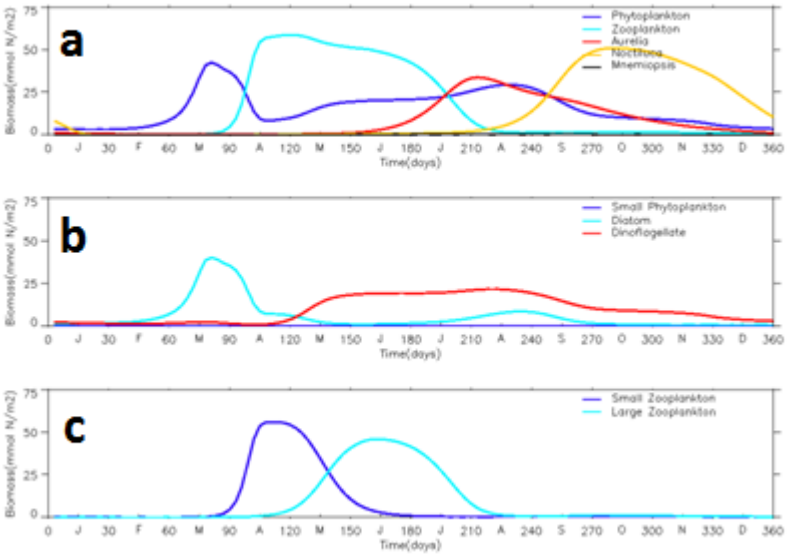

Figure 35. (a) Column integrated biomass of the model compartments,(b) column integrated biomass of phytoplankton groups, (c) column integrated biomass of zooplankton groups with gelatinous carnivores grazing on microzooplankton is reduced by 50%.

3.6.2 Test 2: Mesozooplankton, microzooplankton and total phytoplankton guild

In test 2, the intraguild system where mesozooplankton act as the top predator, microzooplankton acts as the consumer and phytoplankton acts as the prey is analysed. In the first simulation, grazing pressure of mesozooplankton on microzooplankton is reduced. This reduction has weakened the prey-predator relation between mesozooplankton and microzooplankton, thus, food competition became stronger. Results showed that, when the grazing pressure is reduced by 50%, biomass of mesozooplankton and phytoplankton decreased, biomass of microzooplankton increased (Table 6). The increment in microzooplankton biomass is due to reduced grazing pressure exerted by mesozooplankton. High grazing pressure of microzooplankton decreased total phytoplankton biomass. An increment in mesozooplankton biomass was expected when we look at the amount of increment on microzooplankton biomass and decrement in total phytoplankton biomass, total prey of mesozooplankton seem to be increased. But, mesozooplankton prefer feeding on total phytoplankton more than microzooplankton, the decrement in total

phytoplankton biomass affect mesozooplankton more than the same amount of increment in microzooplankton.

In the second simulation, grazing pressure of mesozooplankton on total phytoplankton is reduced. This reduction has weakened the food competition between mesozooplankton and microzooplankton, thus, prey-predator interaction became stronger. Results showed that, when the grazing pressure of mesozooplankton on total phytoplankton is reduced by 70%, mesozooplankton and total phytoplankton biomass decreased, microzooplankton biomass increased (Table 6). The decrement in total phytoplankton biomass shows the effect of weak food competition between mesozooplankton and microzooplankton in favor of microzooplankton. When the food competition is low, microzooplankton feed on total phytoplankton better and increase own biomass. The reason for the decrement in mesozooplankton is the same with the first simulation.

Table 6. Annually averaged mesozooplankton, microzooplankton and total phytoplankton biomass with different gelatinous carnivores grazing preferencies (mmol N m^{-2} day^{-1}).

Simulation	**Mesozooplankton biomass**	**Microzooplankton biomass**	**Total phytoplankton biomass**
Reference	6,17	7,76	15,1
Mesozooplankton grazing on microzooplankton is reduced by 50%	5,5	11,56	13,49
Mesozooplankton grazing on total phytoplankton is reduced by 70%	5,34	11,06	14,07

3.6.3 Top-down Control Mechanism

Three tests have been done to better understand the top-down control mechanism in the model. In the first test, *Aurelia aurita* is removed from the system. In the second test, *Mnemiopsis leidyi* is removed from the system. In the last test, both *Aurelia aurita* and *Mnemiopsis leidyi* are removed from the system.

In the first test, as *Aurelia aurita* eliminated from the system, 2 mmol N m^{-2} decrement in the peak biomass of total phytoplankton, 1 mmol N m^{-2} increment in the peak biomass of microzooplankton, 2 mmol N m^{-2} increment in the peak biomass of mesozooplankton, 5 mmol N m^{-2} increment in the peak biomass of *Noctiluca scintillans* and 4 mmol N m^{-2} increment in the peak biomass of *Mnemiopsis leidyi* were observed (Fig. 36).

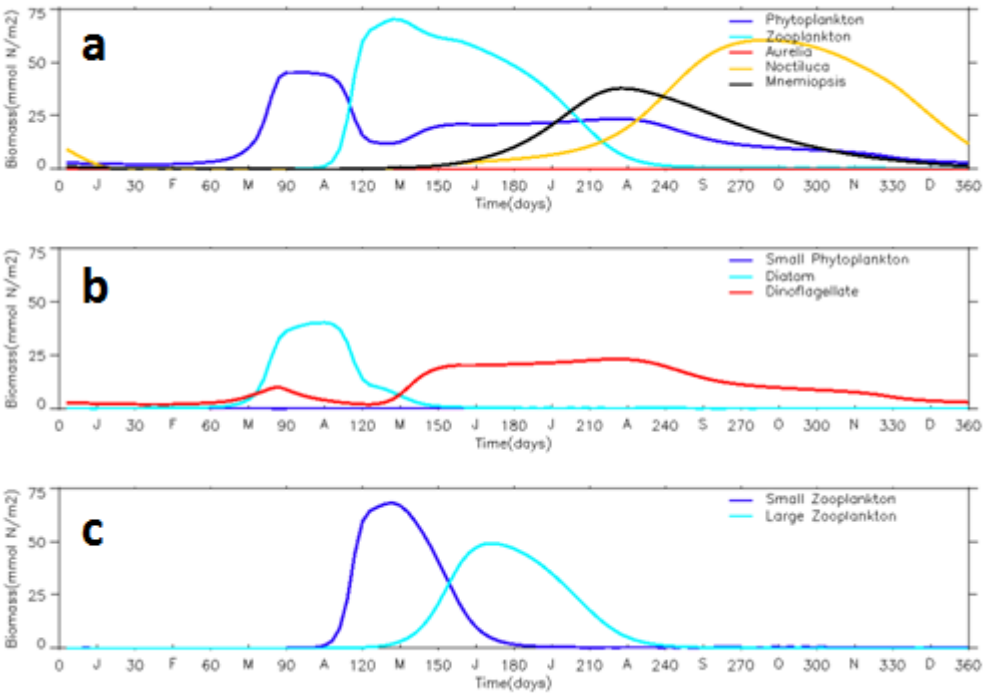

Figure 36. (a) Column integrated biomass of the model compartments,(b) column integrated biomass of phytoplankton groups, (c) column integrated biomass of zooplankton groups without *Aurelia aurita*.

The increment in microzooplankton and mesozooplankton are due to decreased grazing pressure exerted by gelatinous carnivores on them which is a result of eliminating the *Aurelia aurita* from the system. High microzooplankton and mesozooplankton biomass resulted in high grazing pressure on total phytoplankton, thus, decreased total phytoplankton. The increment in the biomass of *Mnemiopsis leidyi* is due to elimination of food competition with *Aurelia aurita*. The increment in *Noctiluca scintillans* biomass is due to the elimination of food competition with *Aurelia aurita* on microzooplankton.

In the second test, as *Mnemiopsis leidyi* eliminated from the system, 5 mmol N m^{-2} increment in the peak biomass of total phytoplankton, 3 mmol N m^{-2} increment in the peak biomass of microzooplankton, 5 mmol N m^{-2} increment in the peak biomass of mesozooplankton, 20 mmol N m^{-2} increment in the peak biomass of *Noctiluca scintillans* and 40 mmol N m^{-2} increment in the peak biomass of *Aurelia aurita* was observed (Fig. 37).

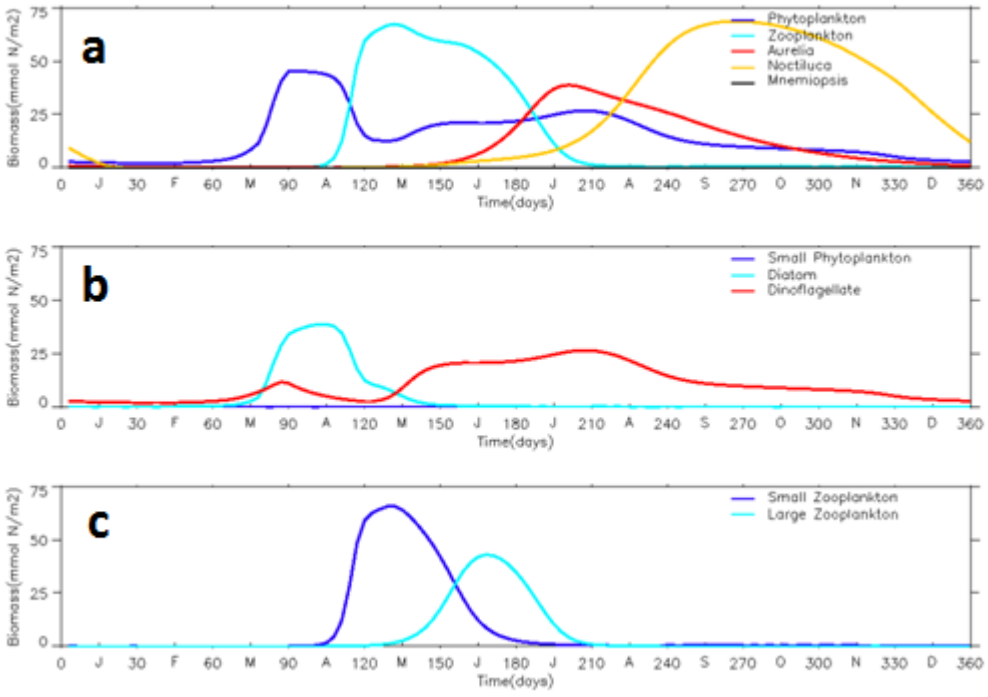

Figure 37. (a) Column integrated biomass of the model compartments,(b) column integrated biomass of phytoplankton groups, (c) column integrated biomass of zooplankton groups without *Mnemiopsis leidyi*.

Mesozooplankton biomass declining to its minimum was observed 45 days earlier as an important shift. The reason of this shift is the dominancy change in gelatinous carnivores. *Aurelia aurita* prefers mesozooplankton more than microzooplankton, however, the preferency of *Mnemiopsis leidyi* is same. When *Aurelia aurita* became dominant in the system, the grazing pressure exerted on mesozooplankton increases significantly.

The reason for the increment in microzooplankton peak biomass is the decreased grazing pressure exerted by the predators. *Noctiluca scintillans* biomass' such increment can also be explained by the change in food preferency of the gelatinous carnivores. Since *Aurelia aurita* prefers less microzooplankton, *Noctiluca scintillans* fed on microzooplankton better.

A decrement in the total phytoplankton biomass was expected; however in this test, we observed and increment in the phytoplankton biomass. This increment may be due to an enhancement in the nutrient cycle in the system as the dominancy in the highest level changed.

In the last test, as both *Mnemiopsis leidyi* and *Aurelia aurita* eliminated from the system, 1 mmol N m^{-2} increment in the peak biomass of total phytoplankton, 10 mmol N m^{-2} decrement in the peak biomass of microzooplankton, 30 mmol N m^{-2} increment in the peak biomass of mesozooplankton, 30 mmol N m^{-2} decrement in the peak biomass of *Noctiluca scintillans* was observed (Fig. 38).

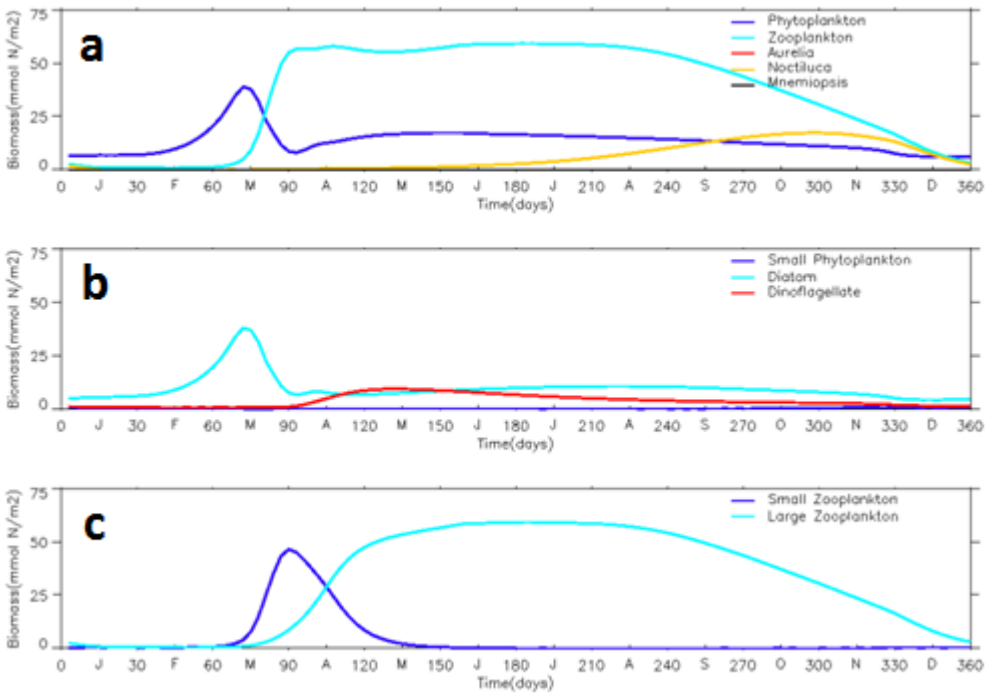

Figure 38. (a) Column integrated biomass of the model compartments,(b) column integrated biomass of phytoplankton groups, (c) column integrated biomass of zooplankton groups without gelatinous carnivores.

In the absence of gelatinous carnivores, mesozooplankton became the dominant top predator as it has a high biomass in 9 months of the year, from early-April till late-December. This is an expected result, because mesozooplankton has no predators in this case. The huge decrement in *Noctiluca scintillans* biomass, the decrements in microzooplankton and total phytoplankton biomass are due to high grazing pressure exerted by mesozooplankton. This result is compatible with what Oguz et al. (2001a) suggested. They suggested that the increased grazing pressure exerted by the gelatinous carnivores results in an increment of phytoplankton biomass indirectly by decreasing the zooplankton biomass.

4 SUMMARY AND CONCLUSIONS

A one-dimensional, vertically resolved, coupled physical-ecosystem model is used to explore the interactions between the main ecosystem components in the Black Sea and to quantify the response of different trophic levels to changing environmental conditions. The fundamental questions addressed were how eutrophication, cold and warm winters influenced the ecosystem. In addition, the prey-predator interactions, food competition and top-down control mechanisms were analysed in detail.

The ecosystem is represented by three groups of phytoplankton (small phytoplankton, diatoms and flagellates), two groups of zooplankton of different sizes (microzooplankton and mesozooplankton), *Aurelia aurita*, *Mnemiopsisi leidyi* and *Noctiluca scintillans* omnivorous dinoflagellates. The proposed structure of the ecosystem is supported by the organic and inorganic (nitrate and ammonium) forms of dissolved nitrogen via the fluxes of suspended and dissolved substances. Although the model used here is based on the model developed by Oguz et al. (2001b), the main focus of Oguz et al. (2001b) was to study the details of the lower trophic levels and their response to changing vertical model resolution. In this study the details of nutrient, phytoplankton, zooplankton and gelatinous carnivores to changing model settings and environmental conditions are analysed.

Results of the reference simulation show that the phytoplankton bloom in the early spring is followed first by the increase in microzooplankton, leading to decrease in the biomass of phytoplankton. Mesozooplankton biomass development followed the microzooplankton bloom as mesozooplankton feed on microzooplankton. The subsequent development of *Mnemiopsis leidyi* biomass reduced the biomass of zooplankton. The maximum intensity of blooming is observed at the end of winter and the beginning of spring as a result of the inflow of biogenic elements into the surface waters caused by winter mixing. Phytoplankton biomass started to increase in the late spring, which led to the permanent growth of the biomass of *Noctiluca scintillans* in late summer until the end of the year. The population of *Mnemiopsis leidyi* started to decrease before *Noctiluca scintillans*, in October. Pronounced and longer periods of blooming of phytoplankton can be linked to *Mnemiopsis leidyi*. Severe regulation of the ecosystem on the upper levels of the trophic chain is the

main reason of this structure. Spring bloom is followed by a persistently high phytoplankton biomass during June to November. Under the influence of *Mnemiopsis leidyi*, the development of *Aurelia aurita* is suppressed throughout the year. The general qualitative agreement of the modeled ecosystem compartments and their seasonal evolution with the observations indicate that the current model can be used for analyzing the long-term changes in the Black Sea. However, it should be noted that the specific features of the dynamics of the basin and intense synoptic variability also affect the biogeochemical processes. Thus, in particular, an important role is played by the transport of waters of the northwest shelf of the sea (rich in biogenic elements) by currents. Without including the circulation dynamics (via a circulation model) it will not be possible to analyse these features.

To carry out a detailed analyses on how the reference model functions, mass flows between ecosystem compartments are computed. Results show that microzooplankton grazing on phytoplankton groups (0.463 mmol N m^{-2} d^{-1}) and nitrate uptake by dinoflagellates (1.234 mmol N m^{-2} d^{-1}) provide the primary pathway for mass (i.e. nitrogen) transfer through nutrients to the primary and secondary producers. Also detailed analyses of model compartments response to changes in the model parameters are performed. Decreasing the half saturation constant in nitrate uptake of dinoflagellates by 20 % resulted in a change in dominant zooplankton (shifted towards mesozooplankton) and gelatinous carnivore type (shifted towards *Aurelia aurita*). The reason for this change is the increase in dinoflagellates biomass. Dinoflagellates are the most preferred food for mesozooplankton and mesozooplankton is the most preferred food for *Aurelia aurita*. Another important result of parameter sensitivity test is the significant decrease in the gelatinous carnivores biomass when the maximum growth rate of mesozooplankton is reduced by 10%. The reason of the decrement in the gelatinous carnivores biomass is the decrease in the mesozooplankton biomass.

The increase of nitrate fluxes, that is used as a proxy of effect of eutrophication, did not change the temporal evolution of model compartments but mainly resulted in an increase of the magnitude of the biomass. For example a 10% increase in nitrate fluxes resulted in an increase of biomass of all levels in the order of 0.5 mmol N (3%) whereas peak biomass of *Noctiluca scintillans* increased by 1 mmol (4%). The

increase in the biomass of the groups is the result of enhanced primary production with increased nutrient. This is the expected result of eutrophication, as described by Oguz et al. (2009b). The reason for a higher increment on *Noctiluca scintillans* biomass is the strength of *Noctiluca scintillans* in the food competition with zooplankton. The general biomass increase of the ecosystem compartments followed a linear trend to further increases in nitrate fluxes.

Winter season temperatures can play an important role on how the seasonal dynamics of the Black sea ecosystem may evolve (Oguz, 2005b, Yunev et al., 2007). However, the observation on the implications of wintertime temperatures on the ecosystem are limited (Mikaelyan, 1997; Niermann et al., 1999; Konovalov and Murray, 2001; Yunev et al., 2002; Lancelot et al., 2002; Daskalov, 2003) and there is an apparent need to study this phenomenon with models, by changing the mixed layer settings in the model, the physical dynamics of the winters are mimicked. In warm winters, the mixed layer shallows earlier than normal winters. This caused lower nutrient supply from bottom to upper layers, thus lower production in the upper, euphotic zone waters. Model results suggested that although the influence of warm winters on the lower trophic levels was minor, the gelatinous organisms highly influenced by this change. A shift from *Mnemiopsis leidyi* dominated system towards *Aurelia aurita* domination occurred. On the other hand, the influence of cold winters on the lower trophic levels was minor, however the *Noctiluca scintillans* highly influenced by this change. Biomass development of *Noctiluca scintillans* started 1 month earlier and the biomass increased with a high rate. The reason for this shift is the increased primary production. Since *Noctiluca scintillans* is stronger in the food competition against zooplankton, higher primary production increased *Noctiluca scintillans* biomass.

Another important result is that, the dominancy of *Mnemiopsis leidyi* in the gelatinous carnivores shifted to the dominancy of *Aurelia aurita*, thus, the equal food preference on mesozooplankton and microzooplankton changed to higher food preference on microzooplankton. The increment on mesozooplankton biomass has 2 reasons; one is the reduced grazing pressure on mesozooplankton due to reduced food preference of gelatinous carnivores on mesozooplankton as the dominancy shifted to *Aurelia aurita*, the other reason is the weakened food competition between

gelatinous carnivores and mesozooplankton, in favor of mesozooplankton. Increment of mesozooplankton biomass increased the grazing pressure exerted by mesozooplankton on microzooplankton, thus, decreased the microzooplankton biomass.

Two main cases of interactions, where a top-predator is feeding on both a consumer and its prey occur in the model. Thus, both prey-predator and competition relationships occur between the top-predator and the consumer. This mechanism is called the intraguild predation theory (IGP) (Holt and Polis, 1996; Polis et al., 1989). In order to analyse the interactions in the system, first prey-predator interaction weakened and then the food competition interaction weakened between the top-predator and predator. In the first case, gelatinous carnivores act as the top predator, mesozooplankton acts as the predator and microzooplankton acts as the prey. When the grazing pressure of gelatinous carnivores on mesozooplankton decreased, the prey-predator interaction between the gelatinous carnivores and mesozooplankton weakens. Such a decrement resulted in increased gelatinous carnivores and mesozooplankton biomass, and decreased microzooplankton biomass. The increment in mesozooplankton is due to reduced grazing pressure, and this increment decreased microzooplankton biomass via prey-predator interaction. The reduction of grazing pressure on mesozooplankton, on the long term, increased the biomass of gelatinous carnivores. When the grazing pressure of gelatinous carnivores on microzooplankton decreased, the food competition interaction between gelatinous carnivores and mesozooplankton weakens. Such a decrement resulted in increased gelatinous carnivores and mesozooplankton biomass, and decreased microzooplankton biomass, however, the dominancy in gelatinous carnivores shifted towards *Aurelia aurita*. Increase in the biomass of mesozooplankton led to an increase in *Aurelia aurita* biomass because *Aurelia aurita* prefers feeding on mesozooplankton more than *Mnemiopsis leidyi* does.

Model is tested by removing top gelatinous compartments from the system. The results were promising in a way that when either *Mnemiopsis leidyi* or *Aurelia aurita* is removed from the system, the remaining gelatinous organism dominated the system, this is in line with the observations (Oguz et al., 2001a). This shows that the

model compartments include sufficient physiological flexibility to adapt to the changing ecosystem structure.

Model results indicate that when the gelatinous carnivores (both *Mnemiopsis leidyi* and *Aurelia aurita)* are removed the mesozooplankton became the dominant top predator and dominated the system during the 9 months of the year. A high decrease in *Noctiluca scintillans* biomass occurred, and decrease in microzooplankton and total phytoplankton biomass is due to high grazing pressure exerted by mesozooplankton. The decrease in total phytoplankton biomass is an important result that shows elimination of the top predators effectively influences the system in a cascading manner as also suggested by Oguz et al. (2001a)

REFERENCES

Arashkevich, E., V. Chasovnikov, V. Kremenetskiy, N. Louppova, S. Mosharov, A. Nikishina, L. Pautova, N. Romanova, A. Sazhin, K. Soloviov, A. Timonin, A. Zatsepin, 2008b. Seasonal dynamics of the NE Black Sea shelf ecosystem. In: Sesame Project 1st Scientific Workshop, 18-20 November 2008, Palma de Mallorca, Spain.

Bingel, F., A.E. Kıdeys, E. Ozsoy, S. Tugrul, Ö. Basturk, T. Oguz, 1993. Stock assesment studies for the Turkish Black Sea coast. NATO-TU Fisheries Final Report, pp. 108, Erdemli-Icel, Turkey.

Bodeanu, N., 1993. Microalgal blooms in the Romanian area of the Black Sea and contemporary eutrophication conditions. In: T. J. Smayda, Y. Shimizu (editors), Toxic phytoplankton blooms in the sea, Elsevier Science Publishers, pp. 203-209, Amsterdam.

Cociasu, A., V. Diaconu, L. Popa, L. Buga, I. Nae, L. Dorogan, V. Malciu, 1996. The nutrient stock of the Romanian shelf of the Black Sea during the last three decades. In: E. Ozsoy and A. Mikaelyan (editors), Sensitivity to change: Black Sea, Baltic Sea and North Sea, NATO ASI Series, Kluwer Academic Publishers.

Codispoti, L., G. Friederich, J. Murray, C. Sakamoto, 1991. Chemical variability in the Black sea: implementations of data obtained with a continuous profiling system that penetrated the oxic/anoxic interface. *Deep-Sea Res.*, **38** Suppl. 2, pp. S691–S710.

Cokacar T., 1996, Comparative Analyses and Seasonal Modelling for the Regional Ecosystems of the Black Sea. Msc Thesis. METU, Turkey

Daskalov, G.M., 2003. Long-term changes in fish abundance and environmental indices in the Black Sea. *Marine Ecology Progress Series*, **25**, pp. 259-270.

Eeckhout, D.V and C. Lancelot, 1997. Modelling the Functioning of the North-Western Black Sea Ecosystem from 1960 to Present. In: E. Ozsoy and A.

Mikaelyan (editors), Sensitivity to change: Black sea, Baltic Sea and North Sea, NATO ASI Series, Kluwer Academic Publishers.

Elbrächter, M. and Y.Z. Qi, 1998. Aspects of Noctiluca (Dinophyceae) population dynamics. In: D.M. Anderson et al. (editors), Physiological Ecology of Harmful Algal Blooms, NATO ASI Series, Vol. G 41, Springer-Verlag, pp. 315-335, Berlin.

Fasham, M.J.R., H.W. Ducklow, S.M. McKelvie, 1990. A nitrogen-based model of plankton dynamics in the oceanic mixed layer, *J. Mar. Res.*, **48**, pp. 591-639.

Hairston, N.G., F.E. Smith, L.B. Slobodkin, 1960. Community structure, population control and competition, *Am. Nat.*, **94**, pp. 421-425.

Holt, R.D. and G.A. Polis, 1996. A theoretical framework for interguild predation. *American Naturalis*t, **149**, pp. 745-764.

Konovalov, S.K. and J.W. Murray, 2001. Variations in the chemistry of the Black Sea on a time scale of decades (1960-1995). *Journal of Marine Systems*, **31**, pp. 217-243.

Konsulov, A., L. Kamburska, 1998. Ecological determination of the new Ctenophora – Beroe ovata invasion in the Black Sea. *Oceanologia*, Vol.2, pp. 195-198, Bulgaria.

Korotaev, G.K., T. Oguz, A. Nikiforov, C.J. Koblinsky, 2003. Seasonal, interannual and mesoscale variability of the Black Sea upper layer circulation derived from altimeter data. *J. Geophys. Res.*, **108** (C4), pp. 3122.

Kovalev, A.V., Yu.A. Zagorodnyaya, N.A. Ostrovskaya, 1996. The investigations of the Black Sea zooplankton in 1995. In: Diagnosis environment state of the Black Sea of coastal and shelves zones, NASU MGI, pp. 254-265, Sevastepol.

Krivosheya, V.G., I.M. Ovchinnikov, A.Y. Skirta, 2002. Interannual variability of the cold intermediate layer renewal in the Black Sea. In: A.G. Zatsepin and M.V. Flint (editors), Multidisciplinary investigations of the northeast part of the Black Sea, Nauka, pp. 27-39, Moscow.

Lancelot, C.L., J.V. Staneva, D.V. Eeckhout, J.M. Beckers, E.V. Stanev, 2002. Modelling the Danube-influenced North-western continental shelf of the Black Sea. Ecosystem response to changes in nutrient delivery by the Danube River after its damming in 1972. *Estuarine Coastal and Shelf Science*, **54**, pp. 473-499.

Lebedeva, L.P. and E.A. Shuskina, 1994. Modeling the effect of Mnemiopsis on the Black Sea plankton community. *Oceanology* (Engl. Transl.), **34**, pp. 72-80.

Mikaelyan, A.S., 1997. Long-term variability of phytoplankton communities in open Black Sea in relation to environmental changes. In: E. Ozsoy, and A. Mikaelyan (editors), Sensitivity to Change: Black Sea, Baltic Sea and North Sea, NATO ASI Series 2: Environment 27, Kluwer Academic Publishers, pp. 105-116, Dordrecht, The Netherlands.

Moncheva S. and A. Krastev, 1997. Some aspects of phytoplankton long-term alterations off Black Sea shelf. In: E. Ozsoy, and A. Mikaelyan (editors), Sensitivity to Change: Black Sea, Baltic Sea and North Sea, NATO ASI Series 2: Environment 27, Kluwer Academic Publishers, pp. 79-94, Dordrecht, The Netherlands.

Murray, J.W., Z. Top, E. Ozsoy, 1991. Hydrographic properties and ventilation of the Black Sea. *Deep Sea Res*., **38**, Suppl. 2A, pp. S663-690.

Mutlu, E., F. Bingel, A.C. Gucu, V.V. Melnikov, U. Niermann, N.A. Ostr, V.E. Zaika, 1994. Distribution of the new invader Mnemiopsis sp. and the resident *Aurelia aurita* and *Pleurobrachia pileus* populations in the Black Sea in the years 1991 – 1993. *ICES J. Mar. Sci.*, **51**, pp. 407-421.

Nesterova, D., S. Moncheva, A. Mikaelyan, A. Vershinin, V. Akatov, L. Boicenco, Y. Aktan, F. Sahin, T. Gvarishvili, 2008. Chapter 5. The state of phytoplankton. In: T. Oguz (editor), State of the Environment of the Black Sea (2001-2006/7), Publications of the Commission on the Protection of the Black Sea Against Pollution (BSC), pp. 421, Istanbul, Turkey.

Niermann, U., A.E. Kideys, A.V. Kovalev, V. Melnikov, V. Belokopytov, 1999. Fluctuations of pelagic species of the open Black Sea during 1980-1995 and

possible teleconnections. In: S. Besiktepe, U. Unluata, A. Bologa (editors), Environmental Degradation of the Black Sea: Challenges and Remedies, NATO ASI Series B: Environmental Security 56, Kluwer Academic Publishers, pp. 147-174, Dordrecht, The Netherlands.

Niiler, P.P., Kraus, E.B., 1977. One dimensional models of the upper ocean. In: E.B. Kraus (editor), Modelling and Prediction of the Upper Layers of the Ocean, Pergamon Press, pp. 143-172, New York

Oguz, T., 2005a. Long term impacts of anthropogenic and human forcing on the reorganisation of the Black Sea ecosystem. *Oceanography*, **18**(2), pp. 112-121.

Oguz, T., 2005b. Black Sea ecosystem response to climatic variations. *Oceanography*, **18**(2), pp. 122-133.

Oguz, T. and B. Salihoglu, 2000. Simulation of eddy-driven phytoplankton production in the Black Sea. *Geophys. Res. Letters*, **27**(14), pp. 2125-2128.

Oguz, T. and D. Gilbert, 2007. Abrupt transitions of the top-down controlled Black Sea pelagic ecosystem during 1960-2000: evidence for regime-shifts under strong fishery exploitation and nutrient enrichment modulated by climate-induced variations. *Deep Sea Res.I*, **54**, pp. 220-242.

Oguz, T., V.S. Latun, M.A. Latif, V.V. Vladimiroc, H.I. Sur, A.A. Makarov, E. Ozsoy, B.B. Kotovshcikov, V.V. Eremeev, U. Unluata, 1993. Circulation in the surface and intermediate layers of the Black Sea. *Deep Sea Res. I*, **40**, pp. 1597-1612.

Oguz, T., H.W. Ducklow, P. Malanotte-Rizzoli, S. Tugrul, N. Nezlin, U. Unluata, 1996. Simulation of annual plankton productivity cycle in the Black Sea by a one-dimensional physical-biological model. *J. Geophysical Research*, **101**, pp. 16585-16599.

Oguz, T., H. Ducklow, P. Malanotte-Rizzoli, J.W. Murray, 1998a. Simulations of the Black Sea pelagic ecosystem by one-dimensional, vertically resolved, physical-biogeochemical models. *Fisheries Oceanography*, **7**(3/4), pp. 300-304.

Oguz, T., H. Ducklow, E.A. Shuskina, P. Malanotte-Rizzoli, S. Tugrul, L.P. Lebedeva, 1998b. Simulation of upper layer biogeochemical structure in the Black Sea. In: L. Ivanov and T. Oguz (Editors), Ecosystem Modeling as a Management Tool for the Black Sea, NATO ASI Series, Environmental Security-Vol.47, Kluwer Academic Publishers, Vol. 2, pp. 257-300.

Oguz, T, L.I. Ivanov, S. Besiktepe, 1998c. Circulation and hydrographic characteristics of the Black Sea during July 1992. In: L. Ivanov and T. Oguz (Editors), Ecosystem Modeling as a Management Tool for the Black Sea, NATO ASI Series, Environmental Security-Vol.47, Kluwer Academic Publishers, Vol. 2, pp. 69-92.

Oguz, T., H.W. Ducklow, P. Malanotte-Rizzoli, 2000. Modeling distinct vertical biogeochemical structure of the Black Sea: Dynamical coupling of the oxic, suboxic and anoxic layers. *Global Biogeochemical Cycles*, **14**(4), pp. 1331-1352.

Oguz, T., H.W. Ducklow, J.E. Purcell, P. Malanotte-Rizzoli, 2001a. Modeling the response of top-down control exerted by gelatinous carnivores on the Black Sea pelagic food web. *J. Geophys. Res.*, **106**, pp. 4543-4564.

Oguz, T., P. Malanotte-Rizzoli, H.W. Ducklow, 2001b. Simulations of phytoplankton seasonal cycle with multi-level and multi-layer physical-ecosystem models: The Black Sea example. *Ecological Modelling*, **144**, pp. 295-314.

Oguz, T., P. Malanotte-Rizzoli, H.W. Ducklow, J.W. Murray, 2002. Interdisciplinary studies integrating the Black Sea biogeochemistry and circulation dynamics. *Oceanography*, **15**(3), pp. 4-11.

Oguz, T., S. Tugrul, A.E. Kideys, V. Ediger, N. Kubilay, 2005. Physical and biogeochemical characteristics of the Black Sea. In: The Sea, Vol. 14, Chapter 33, pp. 1331-1369.

Oguz, T., B. Fach, B. Salihoglu, 2008. Invasion dynamics of the alien ctenophore Mnemiopsis leidyi and its impact on anchovy collapse in the Black Sea. *J. Plankton Res.* **30**(12), pp. 1385–1397.

Oguz, T., V. Velikova, A. Kideys, 2009a. Chapter 12. Overall assessment of the present state of Black Sea ecosystem. In: T. Oguz (editor), State of the Environment of the Black Sea (2001-2006/7), Publications of the Commission on the Protection of the Black Sea Against Pollution (BSC), pp. 421, Istanbul, Turkey.

Oguz, T., V. Velikova, A. Cociasu, A. Korchenko, 2009b. Chapter 2. The state of eutrophication. In: T. Oguz (editor), State of the Environment of the Black Sea (2001-2006/7), Publications of the Commission on the Protection of the Black Sea Against Pollution (BSC), pp. 421, Istanbul, Turkey.

Polis, G.A., C.A. Myers, R.D. Holt, 1989. The ecology and evolution of intraguild predation: potential predators that eat each other. *Annual Review of Ecology and Systematics*, **20**, pp. 297-330.

Salihoglu, B., 1998. A three-layer model of plankton productivity in the Black Sea. Msc Thesis. METU, Turkey

Shapiro, G.I., D.L. Aleynik, L.D. Mee, 2010, Long term trends in the sea surface temperature of the Black Sea. *Ocean Sci.*, **6**, pp. 491-501

Shiganova, T.A., 2000. Some conclusions on studies of intruder *Mnemiopsis leidyi* (A. Agassiz) in the Black Sea. In: S. P. Volovik (editor), Ctenophore *Mnemiopsis leidyi* (A. Agassiz) in the Azov and Black Seas: biology and consequences of the intrusion. AzNIIRKH, pp. 33-75, Rostov-on-Don.

Shiganova, T., E. Musaeva, E. Arashkevich, L. Kamburska, K. Stefanova, V. Mihneva, L. Polishchuk, F. Timofte, F. Ustun, T. Oguz, M. Khalvashi, A. N.Tarkan, 2008. Chapter 6. The state of zooplankton. In: T. Oguz (editor), State of the Environment of the Black Sea (2001-2006/7), Publications of the Commission on the Protection of the Black Sea Against Pollution (BSC), pp. 421, Istanbul, Turkey.

Shuskina, E.A., M.E. Vinogradov, L.P. Lebedeva, T. Oguz, N.P. Nezlin, V.Y. Dyakonov, L.L. Anokhina, 1998. Studies of structural parameters of planktonic communities of the open part of the Black Sea relevant to ecosystem modelin. In:

L. Ivanov and T. Oguz (Editors), Ecosystem Modeling as a Management Tool for the Black Sea, NATO ASI Series, Environmental Security-Vol.47, Kluwer Academic Publishers, Vol. 2, pp. 311-326.

Sorokin, Y.I., 1983. The Black Sea, In: B. Ketchum (editor), Estuaries and Inland Seas, Elsevier, pp. 253–292, Amsterdam.

Stelmakh, L.V., O.A. Yunev, Z.Z. Finenko, V.I. Vedernikov, A.S. Bologa, T.Y. Churilova, 1998. Peculiarities of Seasonal Variability of Primary Production in the Black Sea. In: L. Ivanov and T. Oguz (Editors), Ecosystem Modeling as a Management Tool for the Black Sea, NATO ASI Series, Environmental Security-Vol.47, Kluwer Academic Publishers, Vol. 1, pp. 93-104.

Tugrul, S., O. Basturk, C. Saydam, A. Yilmaz, 1992. The use of water density values as a label of chemical depth in the Black Sea. *Nature*, **359**, pp. 137-139.

Yunev, O.A., V.I. Vedernikov, O. Basturk, A. Yilmaz, A.E. Kideys, S. Moncheva, S. Konovalov, 2002. Long-term variations of surface chlorophyll-a and primary production in the open Black Sea. *Marine Ecology Progress Series*, **230**, pp. 11-28.

Yunev, O.A., J. Carstensen, S. Moncheva, A. Khaliulin, G. Aertebjerg, S. Nixon, 2007. Nutrient and phytoplankton trends on the western Black Sea shelf in response to cultural eutrophication and climate changes. *Estuar. Coast. Shelf S.*, **74**, pp. 63–76.